UNIVERSIDAD POLITÉCNICA DE MADRID
Escuela Técnica Superior de Ingenieros de Caminos Canales y Puertos

Robustness of building floors under column removal. Experimental and theoretical study.

DOCTORAL THESIS

Submitted for the degree of Doctor by:

Yolanda Gutiérrez Diego
Master´s Degree in Materials,
Water and Soil Engineering

Madrid, 2024


UNIVERSIDAD POLITÉCNICA DE MADRID
Escuela Técnica Superior de Ingenieros de Caminos
Canales y Puertos

Doctoral Degree in Engineering of Structures, Foundations and Materials

Robustness of building floors under column removal. Experimental and theoretical study.

DOCTORAL THESIS

Submitted for the degree of Doctor by:

Yolanda Gutiérrez Diego
Master´s Degree in Materials,
Water and Soil Engineering

Under the supervision of:
Dr. Alejandro Pérez Caldentey (Supervisor)

Madrid, 2024

Title: Robustness of building floors under column removal. Experimental and theoretical study.

Author: Yolanda Gutiérrez Diego

Doctoral Programme: Engineering of Structures, Foundations and Materials

Thesis Supervision:

Dr. Alejandro Pérez Caldentey, Civil Engineer (UPM) (Supervisor)

External Reviewers:

Thesis Defense Committee:

Thesis Defense Date:

To my parents. I am what I am because of them

Anyone who stops learning is old, whether at twenty or eighty. Anyone who keeps learning stays young. The greatest thing in life is to keep your mind young. Henry Ford

Publications

Parts of this work have been published as:

2021

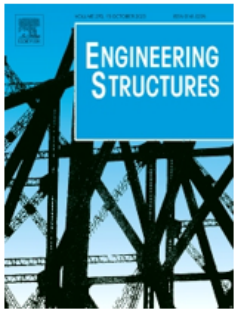

Testing robustness: A full-scale experimental test on a two-story reinforced concrete frame with solid slabs. In *Engineering Structures* Volume 240. Alejandro Pérez Caldentey, Yolanda G. Diego, Freddy Ariñez Fernandez, Anastasio P. Santos.

2023

Experimental response and numerical modeling of a full-scale two-span concrete slab frame subjected to blast load. In *Engineering Structures* Volume 296. Lina M. López, Alejandro Perez-Caldentey, Anastasio P. Santos, Yolanda G. Diego, Ricardo Castedo, María Chiquito.

6th International Conference on Protective Structures (ICPS6), Auburn University USA

Robustness of RC Structures: Conclusions from two full-scale tests and their analysis. Full-Scale test of two-span concrete frame subjected to successive blast loads.

2024

Robustness of RC slab structures: Lessons learned from two full-scale test. *Buildings*, Volume 14, Issue 2 (February 2024). Alejandro Perez-Caldentey, Yolanda G. Diego, Anastasio P. Santos, Lina Lopez, Maria Chiquito and Ricardo Castedo.

Acknowledgement

First, I would like to express my sincere gratitude to my thesis director, Alejandro Pérez Caldentey, for their guidance, support and expertise throughout the entire research process.

I am grateful to the Department of Geological and Mining Engineering of the E.T.S.I. Minas y Energía at UPM, in particular to Tasio Santos, Lina López, Maria Chiquito and Ricardo Castedo who, together with my supervisor Alejandro, conducted the experimental program and were co-authors on the published articles.

Finally, I would like to thank my parents, Avelina and Jose Luis, who always helped and supported me during all the difficulties and challenges I have faced. They are and always be my reference in my life.

Abstract

Within research project ITSAFE, partially funded by the Spanish Government, two full-scale structures were built, one consisting of a single story two-span 7.00.14.00 m2 RC frame with a solid slab and another one consisting of a two-story 7.00x7.00 m2 frame also of RC with solid slabs. In the two-span frame, one of the central supports was first demolished using a pneumatic hammer resulting in rather limited damage (a 14-15 cm deflection at the removed support location).

However torsional cracks appeared at the interface between column and slab at one of the outer supports. When the second central support was removed the structure collapsed due to failure of the support-slab connection. The same type of cracking was observed in the two-story structure, where the column removal was dynamic, and a 22 cm deflection was measured.

From these full-scale experiments, several models of finite elements were developed for the study and analysis of the robustness of the structures. The results were published in three articles and two conferences. This thesis addresses a problem that is not yet resolved in the existing literature, and explain how the loads acting on a slab are resisted after the collapse of a column, in particular how much of the load is resisted by bending and what part is resisted by membrane effect. Existing studies looking at the problem in depth are limited to unidirectional elements, in which they materialize in an artificial longitudinal coercion which allows the axil to be measured and the membrane effect to be evaluated. The problem with real slabs is that there are no external elements that resist an axil, but rather a self-balancing system of axils is formed, which allows the generation of membrane force and the tensile points deform vertically more than the compressed points so the compressions generated at these points allow them to resist greater bending forces. This thesis addresses these issues by relying on the experimentation of the structures on 1:1 scale mentioned above and developed within the scope of the Group of Structural Engineering of the Polytechnic University of Madrid (UPM) and in theoretical analyses using finite elements calculations using LS-DYNA and Sofistik computing programs.

Resumen

Dentro del proyecto de investigación ITSAFE, parcialmente financiado por el Gobierno de España, se construyeron dos estructuras de hormigon armado a escala real, una consistente en una losa de 7.00x14.00 m2 de una sola altura y dos vanos, y otra de dos alturas de 7.00x7.00 m2. En la estructura de dos vanos, una de las columnas centrales se demolió con un martilo neumátio, lo que provocó daños bastante limitados (una deformación máxima de 14-15 cm en la zona de la columna eliminada). Sin embargo, aparecieron grietas debidas a la torsión, en la interfaz entre la columna y la losa en uno de las columnas exteriores. Cuando se retiró la segunda columna central, la estructura colapsó debido al fallo en la conexión losa-columna. El mismo tipo de fisuración se observó en la estructura de dos alturas, donde la eliminación de la columna fue dinámica, y se midió una deformación de 22 cm.

A partir de dichos experimentos a escala real, se desarrollaron varios modelos de elementos finitos para el estudio y análisis de la robustez de las estructuras cuyos resultados se publicaron en tres artículos y dos confenferencias. .

Esta tesis aborda un problema que no está aún resuelto en la bibliografía existente que es explicar cómo se resiste las cargas actuantes en una losa en el caso en que se produzca el fallo de un pilar, en particular qué parte de la carga se resiste mediante flexión y qué parte se resisten mediante efecto membrana. Los estudios existentes que analizan el problema en profundidad se limitan a elementos unidireccionales, en los que se materializa de forma artificial una coacción longitudinal lo cual permite medir el axil y evaluar el efecto membrana. El problema de las losas reales es que no hay un elemento externo que resista un axil, sino que se forma un sistema autoequilibrado de axiles, que permiten generar fuerza de membran en la medida en que los puntos traccionados se deforman en vertical más que los puntos comprimidos y en la medida en que las compresiones que se generan en estos puntos permiten resistir esfuerzos de flexión mayores. Esta tesis aborda estos temas apoyándose en la experimentación de estructuras a escala 1:1 mencionadas anteriormente y desarrolladas en el ámbito de Grupo de Ingeniería Estructural de la Universidad Politécnica de Madrid (UPM) y en análisis teóricos mediante elementos finitos como modelos sofisticados utilizando LS-DYNA y Sofistik.

Contents

List of Figures

List of Tables

Acronyms

ALPs Alternative Load Paths.

DAF Dynamic Amplified Factor.

FEM Finite Element Model.

Chapter 1

Introduction

1.1 Motivation

Within the ITSAFE research project, partially funded by the Spanish Government, two full-scale structures were built, one consisting of a single-story two-story 7x14 m2 RC frame with a solid slab and another one consisting of a two-story 7x7 m2 frame also of RC with solid slabs. In the two-span frame, one of the central supports was first demolished using a pneumatic hammer resulting in rather limited damage (a 14-15 cm deflection at the removed support location). However, torsional cracks appeared at the interface between the column and the slab at one of the outer supports. When the second central support was removed, the structure collapsed due to failure of the support-slab connection. The same type of cracking was observed in the two-story structure, where column removal was dynamic, and a 22-cm deflection was measured.
When a column of a concrete slab is lost due to an accidental or an attack event, the forces of the tensile membrane can be activated. These forces can greatly enhance the load capacity of the slab compared to predictions based on small deformation theories that ignore the effects of the membrane. This mechanism can help prevent progressive collapse and significantly improve the robustness of concrete structures. Understanding and utilizing this phenomenon is critical to evaluating the strength reserve and resilience of such structures. In accidental scenarios, the risk of structural failure increases, leading to large deformations. To date, relatively few large-scale tests have been conducted to study the behavior of the tensile membrane in concrete slabs. Large-scale tests are costly and time consuming; therefore, numerical modeling of the tensile membrane effect is essential. These numerical models need to be validated through an experimental full-scale test. Despite the need for full-scale tests of two-way concrete slabs, most research to date prioritized studying the behavior of the tensile membrane in one-way slabs. Gouverneur in his doctoral thesis (Gouverneur, 2014) elaborated an experimental program to investigate the action of the tensile membrane in a one-way restricted concrete slab. The developed slabs were a four-span reinforced slab strip of 1800 mm wide, 140 mm, and 160 mm thick, and a total length of 14.3 m. The distance between the inner supports and the central one was 4 m, and the spans changed to a span of 8 m after controlled removal of the center support to simulate an accidental event. The

slabs were horizontal restrained and displacement controlled loaded until failure. In this way, due to the increase in the load and consequently the vertical deflection, the forces of the tensile membrane were activated because of the horizontal restraining system. This type of approach to the study of the membrane effect does not take into account the dynamic effects, the unrestraint systems, or the two-way redistribution of the forces after a column removal, which are present in real structures. Due to this lack of research, this thesis focuses on the analysis of two-way full-scale concrete slabs without restrictions.

1.2 Goals and Objectives

Criticism of the use of strut and tie rod models as an exclusive model for analysis. Both tests and finite element analyses have shown that the collapse of the structure can be achieved by premature breakage, by torsion, of the slab/support interface. This aspect is not considered in strut and tie rod models and its application as an exclusive tool for analysis can be unsafe. On the other hand, strut and tie rod models are very useful for identifying certain geometries where it is not possible to obtain balance after the breakage of a support, mainly because when a break line crosses the crank, a resultant directed downwards is produced. In these cases, the only possible balance is that the supports have sufficient resistance capacity to anchor the forces of the tie rods. This will only be possible in large-scale buildings with many columns.
Study of the fundamental differences between the behavior of one-dimensional elements (which are the subject of a very important percentage of the robustness studies available in the literature) that are assumed to be longitudinally anchored and the two-dimensional elements that require the formation of self-balancing force systems.

1.3 Document Structure

This thesis is structured as follows:

Chapter 1: Introduction, describes the motivation of the thesis, the goals to achieve, and the objectives set to achieve the goals.

Chapter 2: State of Art, where the relevant studies done at this time are analyzed.

Chapter 3: Finite Element Modeling. This chapter introduces the background and details of the numerical models used to simulate the structures.

Chapter 4: A validation of the Finite Element Model using the modeling approach outlined in Chapter 3, and incorporating measured material properties and defined geometries, to compare finite element results with corresponding experimental outcomes.

Chapter 5: Numerical Investigation of membrane forces using different tools.

Chapter 6: A detailed analysis of the resistance mechanisms for robustness of structures.

Chapter 7: Conclusions and future works, summarize the contribution of this thesis and describe current and future research lines to continue the work that was initiated through this thesis.

Reference section, which shows a list of codes and publications related to the work of this thesis.

And finally, the Annex section, which includes the cover of the publications fulfilled during the development of this thesis.

Chapter 2

State of Art

2.1 Historical studies

Public and private buildings of all types may be subjected to extreme events caused by earthquakes, explosions, tsunamis, fires, vehicle impacts or terrorist attacks. These events cause local damage to the structure and this can lead to a complete collapse. Progressive collapse refers to the spread of an initial local failure in a structure, leading to the collapse of the entire building or a large part of it. Progressive collapses, are a principal cause of injury and death in building failures. Ellingwood, 2006

During World War II (WWII), some of the U.K.´s leading research engineering including John Baker, found that designs should account for the actual failure mechanism of the structure, and this discovery led to the development of plastic methods of analysis, some of which were used for designing air raid shelters during WWII Smith et al., 2010.

Later at the end of the 70´s, a gas explosion on the $18th$ floor of the 22-story Ronal Point apartment tower in Newham (London), caused the loss of support near the corner of the building. This caused the floors above to collapse and set off a chain reaction that ended up with the failure of all the corner bay of the building, as can be seen in figure 2.1.

After this event, the concept of Robustness was coined. Eurocode 1 in Part 1.7 Vrouwenvelder, 2005. This code defines the concept of Robustness as follows:

"the ability of a structure to withstand events like fire, explosions, impact, or the consequences of human error, without being damaged to an extent disproportionate to the original cause"

Figure 2.1: The Ronan Point disaster, 1968. Source:©London Borough of Newham - Heritage &Archives

This type of sequential failure was named "progressive collapse" and after this event, the engineering community and public regulators decided to change the practice of building design in order to avoid this kind of disasters.

The following graph it can be seen the evolution in the number of natural disasters since 1970 until 2020 and a specked trend for the coming 10 years. The trend shows an increase of disaster events by 40% in 2030 year.

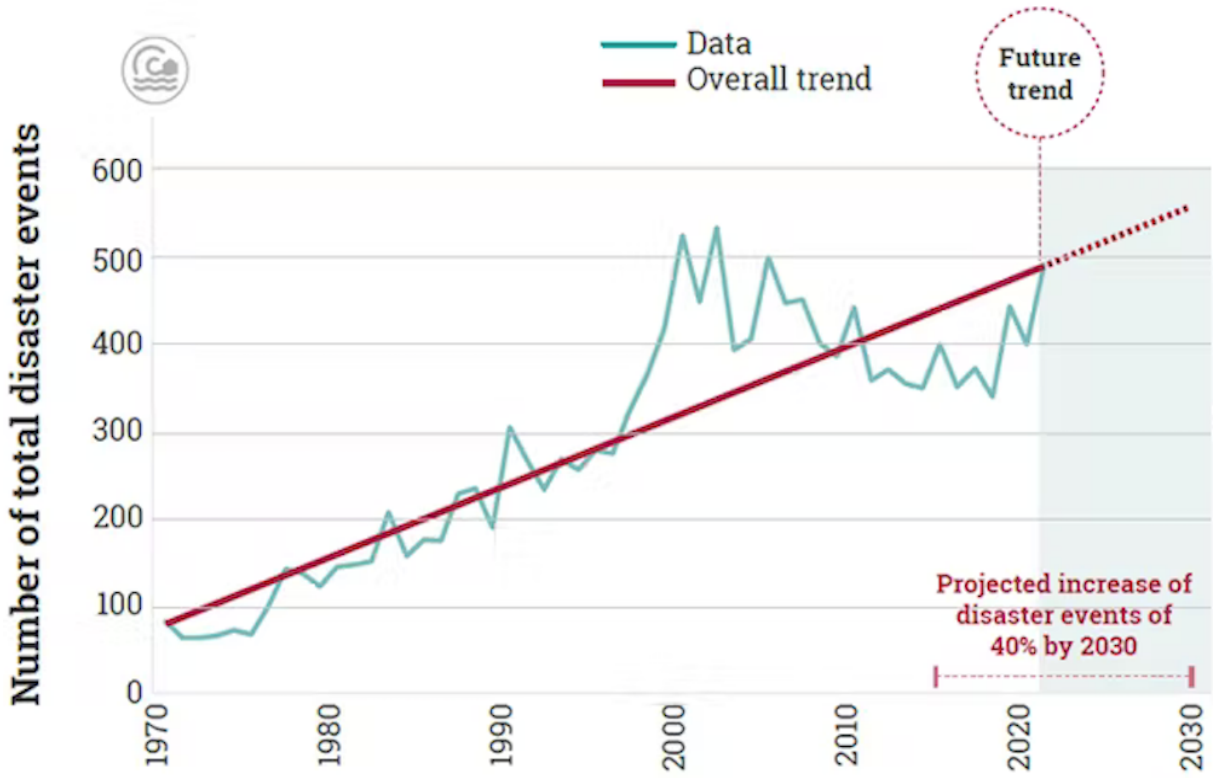

Figure 2.2: Number of total disaster events (Data from EM-DAT, 2021)

The following figures shown the classification and the number of natural disasters in the last twenty years and the consequences of these events. The number of total deaths and the economic losses are almost twice comparing the dates between 1980-1999 and 2000-2019.

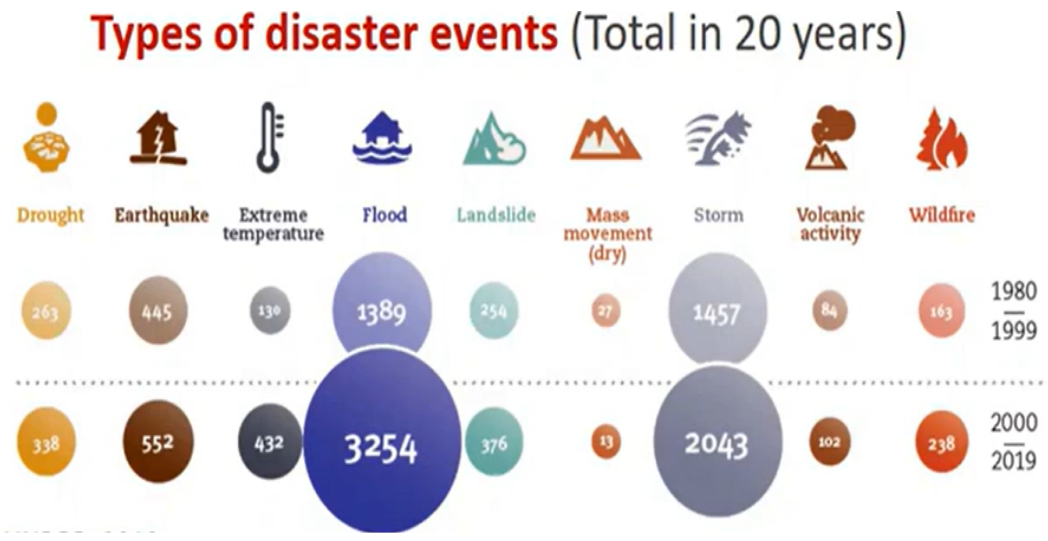

Figure 2.3: Types of disaster events (UNDRR, 2019)

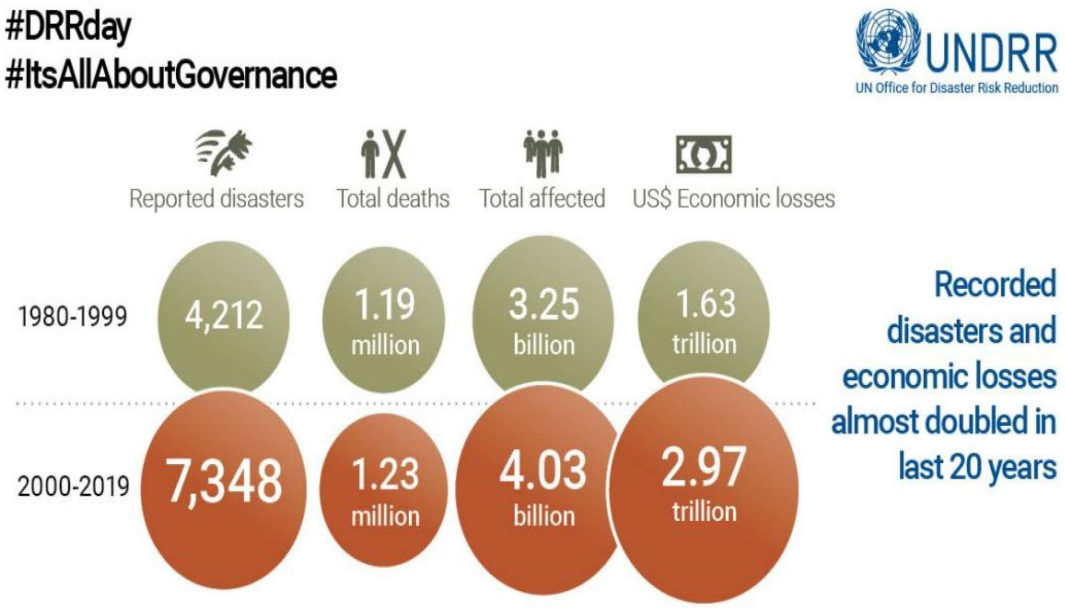

Figure 2.4: Cost of the consequences of disaster events in the last years (UNDRR, 2019)

On 19 April 1995, the Murrah Federal Building in downtown Oklahoma City was destroyed by a bomb located inside a truck parked at the base of the building. The bomb destroyed or badly damaged three columns. This loss of support led to failure a transfer girder. And this caused the collapse of columns supported by the girder and the floor areas that were sustained by the columns. As a result, a big area of the building collapsed as can be seen in figure 2.5. The collapse of this structure was a clear example of a progressive collapse in the entire terms:

"Disproportionate collapse or progressive collapse occurs in a building when the failure of one component leads to the progressive failure of a series of other components, often with catastrophic results"

Figure 2.5: Alfred P. Murrah Federal Building in Oklahoma City on April 19, 1995

On September 11, 2001, two Boeing 767-200ER commercial aircraft hit the World Trade Centre buildings killing over 2800 people in the biggest terrorist attack on the United States. The two towers experienced a similar, but not identical, series of loading events. The sequence of the events was the same for the two buildings, although the timing was not. In the first event, the aircraft impacts resulted in severe structural damage in each case, including some localized partial collapse. The second was the ignition of the fuel and the growth of fires over several floors and different zones of the buildings. The fires heated the structure, causing stresses on a structure previously damaged by aircraft impacts and causing a loss of strength that started the third event, a progressive sequence of failures that ended up in the collapse of both towers.

Figure 2.6: World Trade Center Towers, 2011.Source:©Roberto Rabanne

This event was an example of progressive collapse, where a pancake type collapse mechanism led to progressive failure of the structure and ended with the complete destruction of the towers. After these two big attacks, an alarmed public opinion led to the introduction of new standards and recommendations.

In 2006, Terminal 4 of Madrid‘s Airport was hit by a terrorist attack. A van bomb parked in the second floor of the car park, on module D exploded. The explosion demolished almost all the five floors of the car park and produced tones of debris. After the explosion, the failure of

the connection between supports and slabs was caused by load inversion Bermejo et al., 2015.

Figure 2.7: T4 Terminal, Madrid Airport, 2006

It is difficult to predict the probability of occurring and the magnitude of a terrorist attack or other kind of extreme events, and it is no practical or possible to design structures against them using the traditional methods for conventional loads. Current designs standards try to minimize the risks and incorporate the concept of robustness as the insensitivity of a structure to local damage. Adam et al., 2018

Two new standards from ASCE's Structural Engineering Institute offer critical provisions for civil engineers planning, designing, constructing, or assessing buildings. ASCE 59-22: Blast Protection of Buildings considers the effects of accidental or malicious explosions on buildings of Civil Engineers, 2023a, while ASCE 76-23: Standard for Mitigation of Disproportionate Collapse Potential in Buildings and Other Structures, describes the minimum requirements for all phases of building design and construction related to disproportionate collapse of Civil Engineers, 2023b.

2.2 Definitions

There is no unique definition of what represents a progressive or disproportionate collapse Haberland and Starossek, 2009. Two concepts established the difference between both definitions. The concept of disproportion between the cause and the effect, and the concept of failure progression or chain reaction. According to these concepts, it is possible to distinguish progressive and disproportionate collapse. If there is a pronounced disproportionate collapse between a relatively minor event and the collapse of a major part or even the whole of the structure, then is a disproportionate collapse. When the collapse start with the failure, initiated by a triggering event, of one or few structural components which then started a chain of successive failure of other components not directly affected by the initial even, then is a progressive collapse Starossek, 2009.

Some definitions of progressive and disproportionate collapse are listed in 2.1.

Source	Definition of progressive and disproportionate collapse
ASCE (2005)	Progressive collapse is defined as the spread of an initial local failure from element to element resulting, eventually, in the collapse of an entire structure or a disproportionate part of it.
GSA (2003)	A progressive collapse is a situation where local failure of a primary structural component leads to the collapse of adjoining members, which, in turn, leads to additional collapse. Hence, the total collapse is disproportionate to the orignal cause.
UFC 4-010-01 (DoD 2003)	Progressive collapse. A chain reaction failure of building members to an extend disproportionate to the original localized damage.
Agarwal and Englad (2008)	Disproportionate collapse results from small damage or a minor action leading to the collapse of a relatively large part of the structure. Progressive collpase is the spread of damage through a chain reaction. Often progressive collapse is disproportionate but the converse may not be true.

Table 2.1: Definitions of the terms progressive collapse and disproportionate collapse

The robustness expression play a part in publications regarding progressive or disproportional collapse. But there is no general agreement to its precise meaning Haberland and Starossek, 2009. A selection of robustness definitions is listed in 2.2.

Source	Definition
Eurocode 1 Part 1-7, 2006	The ability of a structure to withstand events like fire, explosions, impact of the consequences of human error without being damaged to an extend disproportionate to the original cause
ASCE 7 2010	The spread of an initial local failure from element to element, eventually resulting in the collapse of an entire structure or a disproportionately large part of it
Smilowitz and Tennant 2001	Progressive collapse occurs when an initiating localized failure causes adjoining members to be overloaded and fail, resulting in an extent of damage that is disproportionate to the originating region of localized failure.
Ellingwood 2006	A progressive collapse initiates as a result of local structural damage and develops, in a chain reaction mechanism, into a failure that is disproportionate to the initiating local damage.
Mohamed 2006	Progressive collapse of building structures is initiated by the loss of one or more load-carrying members. As a result, the structure will seek alternate load paths to transfer the load to structural elements, which may or may not have been designed to resist the additional loads. Failure of overloaded structural elements will cause further redistribution of loads, a process that may continue until stable equilibrium is reached. Equilibrium may be reached when a substantial part of the structure has already collapsed. The resulting overall damage may be disproportionate to the damage in the local region near the lost member.
Adam et al. 2018	Progressive collapse is a collapse that begins with localised damage to a single or a few structural components and develops throughout the structural system, affecting other components.
Li et al. 2019	Building robustness to progressive collapse can be generally defined as a measure of the ability of a system to remain functional in the event of the local failure of a single component or multiple connected components.

Table 2.2: Definitions of the term robustness

Recapitulating these definitions, robustness involves the ability of a structure no to respond disproportionately to either abnormal events of initial damage.

According to Starossek, 2009, a structure is collapse resistant if an abnormal event does not lead to disproportionate collapse.

A commonly associated concept with structural robustness is "redundancy." Redundancy in a structure generally refers to its capacity to redistribute loads to other components when one or more members are damaged. Frangopol and Curley, 1987 describe "redundancy" as the presence of multiple load-bearing paths within a structure or the absence of critical elements whose failure could lead to collapse. When certain structural elements are compromised, the

remaining redundant components should be able to transfer the loads that were originally supported by the damaged elements, thereby preventing disproportionate damage. Similarly, Starossek and Haberland, 2010 defines "redundancy" as the availability of alternative load paths. Adam et al., 2018 suggests that a robust structure is not necessarily over-designed, but rather one that can activate alternative resistance mechanisms to minimize the impact of an initial damage event. Kanno and Ben-Haim, 2011 define "redundancy" and "robustness" as the extent to which a structure can endure damage without losing specific functionalities and the extent to which it can maintain functionality under environmental uncertainty, respectively. Although these concepts are closely related, Starossek and Haberland, 2010 defines "vulnerability" as the susceptibility of a structure to suffer initial damage when affected by abnormal events. This concept is echoed in the report by the Joint Committee on Structural Safety (JCSS) Narasimhan and Faber, 2009, where "vulnerability" is understood as the direct impact of an abnormal event on a component's behavior. To enhance a structure's resistance to collapse, its vulnerability can be reduced by either protecting the component or increasing its resistance. Therefore, "vulnerability" is linked to the behavior of individual components, while "robustness" refers to the performance of the entire system.

2.3 Types of progressive collapse

There are various forms of progressive collapse, each identified by how the failure progresses through a structure. The primary types include pancake, zipper, domino, section, instability, and mixed forms Elkady et al., 2024

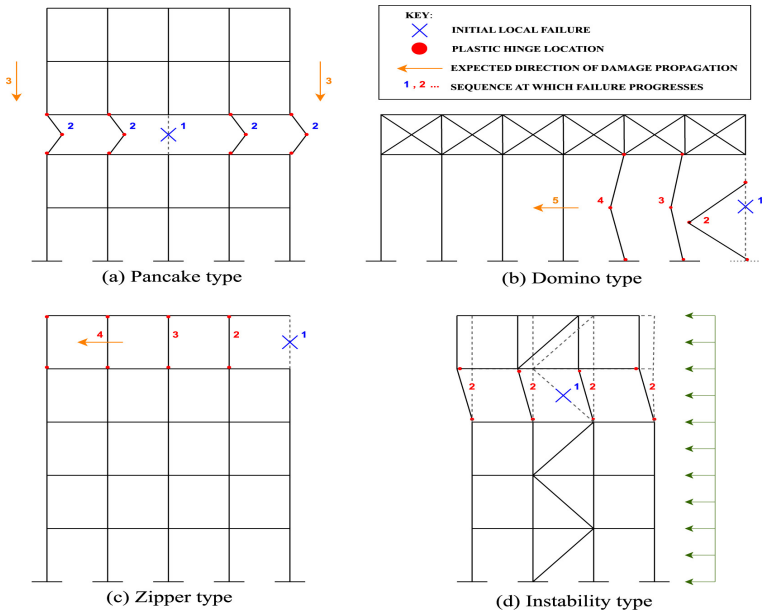

Figure 2.8: Different collapse mechanisms (Source:©Elkady et al.)

Figure 2.8 illustrates the most frequent progressive collapse types. These can be organized into broader categories based on the underlying collapse mechanisms. For instance, pancake and domino collapses fall under the impact category, as they result from the rapid conversion of the failed elements potential energy into kinetic energy. Additionally, zipper and section collapses are part of the redistribution category, occurring largely due to the shift of forces from failed components to other parts of the structure.

2.3.1 Pancake collapse

The main trigger for a pancake type collapse is a reduction in vertical load bearing capacity due to an abnormal event, such an explosion, fire or accident. This leads to the failure of structural members, which begin to fall as debris onto the components of lower floors. This event triggers the failure of structural members, which then fall as debris onto lower floors, subjecting them to high dynamic impact loads. In man cases, these loads can reach up to four times the static loads for which the floors were originally designed, leading to their collapse Lalkovski and Starossek, 2014. This type of collapse is especially common in high rise buildings. Even these type of buildings are designed with redundancy and can create alternative load paths, if column fails, the structure cannot prevent this type of progressive collapse. This inability is likely due to the increase in debris and impact forces with the number of floors in the structure. The failure of the WTC Twin Towers is the best example of a pancake type collapse. After the initial impacts, fires, structural failures and the falling debris accumulated kinetic energy that could not be dissipated, causing the floors below of the impact, a sequentially collapse Starossek, 2007. Pancake type collapse can also occur in low rise buildings, typically featuring vertical failure propagation and punching shear failures in slabs. To enhance the resilience of a building against this type of collapse, solutions like energy absorption devices can be employed Zhou and Yu, 2004.

2.3.2 Domino collapse

This type of collapse is other form of impact collapse Bi et al., 2015. In this case, an initial event causes a structural member to fail, which then impacts an adjacent member laterally, leading to a similar failure. This process continues, spreading the collapse to nearby members. The key difference between domino type and pancake type collapse lies in the direction of the forces driving the collapse. In domino collapses, these forces, as gravity, act perpendicular to the direction of failure propagation Starossek, 2009. In contrast, pancake collapses are driven by forces that run parallel to the direction of collapse progression. Due to its specific mechanism, domino type collapse is more common in bridges or horizontal structures, often triggered by the failure of piers or other slender supports Kiakojouri et al., 2020. A notable example is the collapse of a wooden trestle railroad bridge in Texas in 2013. The fire in the bridge started in one of the wooden trestles, causing it to collapse and impact adjacent members, ultimately resulting in the complete collapse of the structure. This type of failure can be mitigated by reinforcing or retrofitting structural members to withstand loads that may be transferred from neighboring members in the failure event.

Figure 2.9: Texas wooden trestle railroad bridge fire

2.3.3 Zipper collapse

This type of progressive collapse is a form of redistribution collapse that occurs when an Alternative Load Path (ALP), designed to carry redistributed loads in the event of a member failure, also fails Kiakojouri et al., 2020. This collapse type if often triggered by the sudden demand for dynamic load redistribution rather than by impact loads, which play a less significant role in zipper collapses. The failure of the top floor at Pipers Row Car Park in the UK in 1997 is an example of this type of collapse. In this case, one column punched through the top floor slab, forcing the load onto adjacent columns, which could not sustain the increased load and ultimately failed as well Starossek, 2009.

2.3.4 Section collapse

Section collapse represents a form of redistribution collapse, similar in concept to zipper collapse, but specific to element sections. This collapse occurs, for instance, in a tensioned bar where the failure of a cross-section propagates to adjacent parts of the same element due to insufficient load redistribution. Section collapse typically affects continuous, single elements like cables or shells rather than systems made up of discrete, connected units. Due to this sudden, interdependent nature, this failure often manifests as a rapid fracture rather than a gradual, progressive collapse Starossek, 2009. This type of collapse is one of the more frequently observed collapse due to the wide range of structural configurations that can be impacted.

2.3.5 Instability collapse

This type of collapses occur when structural components, primarily designed to stabilize the structure, fail. Bracing is a key example of such a component; for instance, in pinned steel

frames, bracing is essential to maintain stability under lateral loads. If the bracing fails, the structure becomes unable to resist lateral forces, leading to collapse. Instability failures may result in either immediate or progressively disproportionate collapses, depending on the function and location of the damages element Starossek, 2009.

2.3.6 Mixed type collapse

In real world structural failures, it is rare for only one type of collapse to occur; instead, mixed type collapses are more common Kiakojouri et al., 2020. Despite limited research on categorizing and analyzing combined collapse types, several well known incidents illustrate these complex failure mechanisms. According to Starossek, 2009, collapse of the Samppoong Superstore in Seoul in 1995, exemplifies a mixed type failure : it began with columns punching through the slabs. as the load was redistributed, the failure propagated horizontally, inducing a zipper type collapse, ultimately leading to a loss of vertical load bearing capacity in the slabs and causing a pancake collapse.

Figure 2.10: Sampoong Superstore collapse. Source:©AFP—Choo Youn-Kong/Getty Images

WTC 7 is another case of mixed type collapse. Although the exact causes remain under investigation, the National Institute of Standards and Technology (NIST) attributes the likely failure to thermal expansion, which may hae displaced a girder from its supporting column. This triggered a pancake failure of the floor area supported by that girder and led to lateral support loss and buckling in the associated column. This failure caused load redistribution to other structural members with large spans, resulting in a zipper type collapse. The combination of these failure modes rapidly spread through the building, leading to a total collapse within seconds. Figure 2.11 shows how thermal expansion led to the collapse of World Trade Center Building 7 (WTC 7) Nist, 2013.

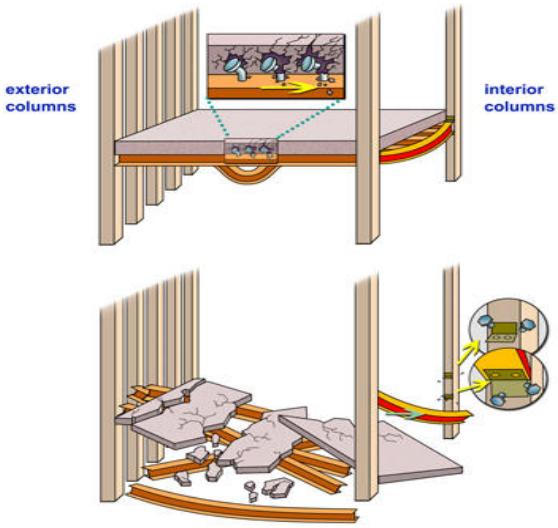

Figure 2.11: WTC 7 NIST graphic (credit:Loel Barr)

2.4 Progressive collapse standards

Relatively few Codes of Practice (CoPs) currently provide explicit guidelines for structural robustness, although those that do are regularly updated to reflect advancing research and best practices. The United Kingdom's response to the 1969 Ronan Point collapse market the introduction of its first structural robustness requirements, established through the Fifth Amendment of the Building Regulations (Minister of Housing and Local Government, 1970). These regulations sought to ensure that buildings could redistribute loads and maintain stability following a local failure, thus introducing the principle of notional member removal. Over time, this concept evolved into a variety of methodologies now embedded in contemporary international codes, with present-day design standards reflecting a direct progression from the foundational guidelines introduced in the Fifth Amendment.
In the United States, the Ronan Point collapse similarly initiated research at the National Bureau of Standards and fostered technical discussions on progressive collapse in the 1970s. During this period, concerns emerged within the engineering community that the increasing focus on structural optimization and accelerated construction timelines could compromise robustness, potentially elevating the risk os progressive collapse when exposed to unforeseen loads.
The 1996 bombing of the Khobar Towers complex in Saudi Arabia, which housed U.S. Department of Defense (DoD) personnel, served as a further catalyst, prompting Congress to mandate the development of anti-terrorism constructions standards for DoD buildings. These standards aimed to reduce structural vulnerabilities to terrorist threats and enhance occupant protection. In response, the DoD issued interim design guidelines in 2001, which specifically addressed progressive collapse using an alternate load path methodology aligned with emerging GSA citeria (DoD, 2001).

In 2002, the DoD expanded its anti-terrorism provisions by issuing Unified Facilities Criteria (UFC) 4-010-01, which introduced requirements for progressive collapse mitigation (DoD, 2002). This was followed by UFC 4-023-03 in 2005, offering comprehensive design guidance to meet the UFC-4-10-01 standards. This guidance underwent further revisions in 2009 (DoD, 2009). In other countries, explicit structural robustness provisions did not appear in building codes until the early 21st century. For example, following the widespread building failures during the 2008 Wenchuan earthquake, China introduced the Code for Anti-Collapse Design of Building Structures in 2014. Sanctioned by the Ministry of Housing and Urban-Rural Development, this code aligns with international standards for steel and concrete structural design (China Association for Engineering Construction Standardization.
The 1995 bombing of the Alfred P. Murrah Federal Building in Oklahoma City also influenced structural security guidelines in the U.S., leading to the formation of the Interagency Security Committee (ISC). This committee developed security standards for federal facilities requiring blast resistance and other protective features. Following extensive evaluations of progressive collapse mitigation strategies, the General Services Administration (GSA) adopted the "alternate path" approach in 2000. This approach is designed to enhance structural robustness by providing reserve capacity and ductility, enabling building to sustain gravity loads even in the absence of a key structural member.
By 1975 the National Building Code of Canada (National Research Council of Canada, 1975) had introduced explicit provisions aimed at preventing progressive collapse. As observed Ellingwood, 2006, the Canadian code is notable for setting specific thresholds for acceptable probabilities of progressive collapse, establishing a distinct framework for structural safety requirements.However, from 1975 to 1995, progress in this area stalled due to a lack of interest within the structural engineering community.
In Australia, significant code updates regarding structural robustness were made only in 2016. The revised code introduced basic requirements, including concepts like notional member removal and key element design, applicable to all building types (Australian Building Codes Board (ABCB), 2016).
In 2004, the European standard EN 1991-1-7 CEN et al., 2004, was completed and received approval from the member states. This standard provides guidelines for assessing accidental actions on buildings and bridges. Its key design principle is that local damage is acceptable as long as it does not threaten the overall stability of the structure and that the load-bearing capacity is preserved for a sufficient period to facilitate emergency response Gulvanessian and Vrouwenvelder, 2006.
Eurocode 1991-1-7 introduced the concept of notional column removal as well as the idea of introducing properly anchored ties between support lines with the idea of preventing total structural collapse as a result of the loss of column by mobilizing membrane forces within the deformed slab.

2.5 Column removal concept

Concrete structures subjected to the loss of a column, when they are properly designed, can be able to find a different equilibrium path from the bending for which it was design by mobilizing membrane forces in the slab. This strategy is involved on the strategies for accidental design situations considered in EN 1991-1-7 Eurocode Standard, 2006 as can be seen on Figure 2.12.

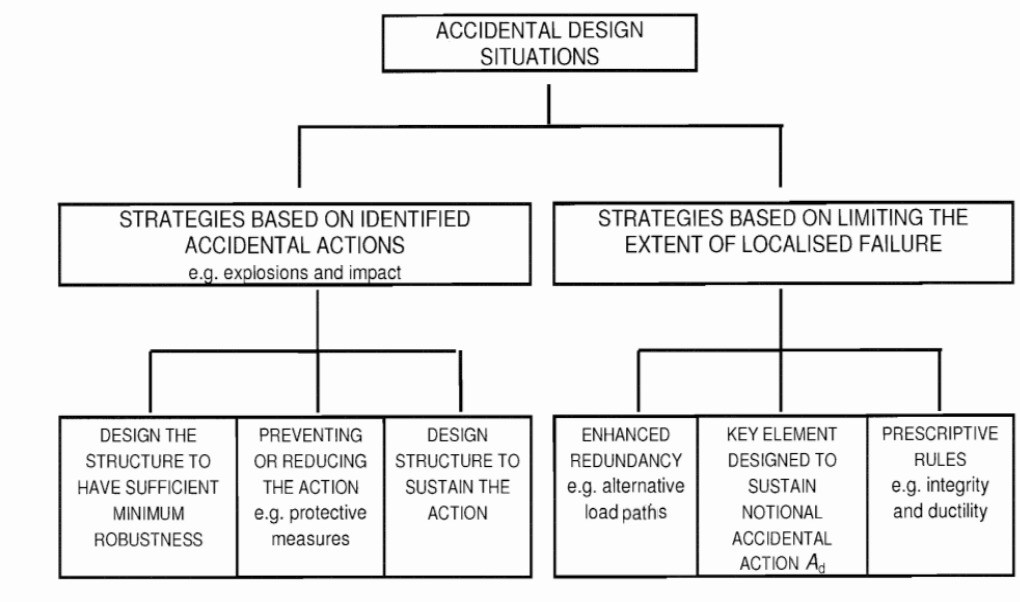

Figure 2.12: Strategies for Accidental Design Situations EN1997-1-7 Eurocode 1

The main objective is to increase the membrane capacity so that the local collapse of a member can be absorbed through a redistribution process, that can exploit the membrane effect (see Figure 2.13).

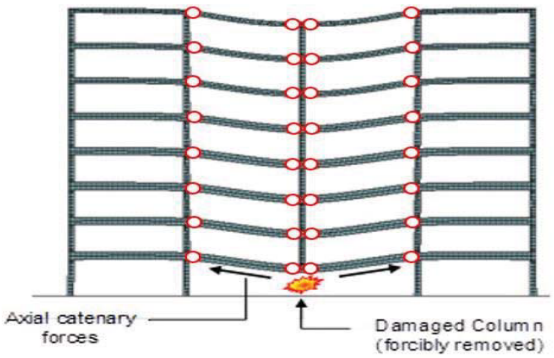

Figure 2.13: Development of the catenary effect following the removal of a column (from http://www-personal.umich.edu/ eltawil/catenary-action.html)

The concept of the membrane forces within the deformed slab after a column removal remains however, dubious because of the lack of background information and also to the reasonable doubts showed by structural engineers as to whether real concrete structures can be made to develop deflections close to 1.00 meter and still retain the ability to resist loads.

After the instantaneous removal of a column, compressive forces in the columns above the one removed will vanish in milliseconds and these forces will be redistributed to the surrounding supports. The dynamic gravity loads redistributed, are supported by the horizontal structural parts, going over the removed column and deflecting until the equilibrium is reached. If the equilibrium is not possible or the vertical load bearing parts of the structure fail due to the additional compression forces, the collapse of the structure will occur. Even so, columns are generally capable to assume this increase and therefore, only the behavior of the horizontal components of the structure and the connection with the columns are relevant for the robustness of the structures.

After the sudden loss of a column, the response of the structure is highly complex and involve structural dynamics and geometrical and material nonlinearities due to the expected large displacements (Müllers, 2007). Until now, a relative small number of full scaled experimental tests on concrete structures are available in the bibliography. The influence of cracking, ultimate rotation capacity, boundary conditions and material properties needs a deeper scientific research. In following section, some of previous research on compressive membrane is described.

2.5.1 Corner removal scenarios

Previous analytical work, on membrane action in unrestrained slabs, has been presented by Wood, 1961, Taylor, 1965, Kemp, 1967, Sawczuk and Winnicki, 1965 and Hayes, 1968. Wood´s analysis was limited to circular slabs. Both Taylor and Kemp ignored the development of the large crack forming across the shorter span of the slab and thus typically overestimated the load-carrying capacity of the slab C. G. Bailey, 2001. Sawczuk and Winnicki, 1965 presented and energy method including the formation of large cracks along the shorter span. They considered two models of failure (see Figure 2.14) Sawczuk shown theoretically that the critical mode of failure was caused by these large cracks formed along the shorter span, at the intersection of the yield lines (mode (i) in Figure 2.14). Using as a base the theoretical derivation developed by Hayes, 1968, C. G. Bailey, 2001 and C. Bailey and Toh, 2007 expanded the model that correspond to the (ii) mode of failure in Figure 2.14 since model (i) "contradicts a large portion of the test results" C. G. Bailey, 2001. Inspection of the theoretical method shows that Sawczuk assumption of full tensile membrane action occurring in the central area of the slab is typically non conservative C. G. Bailey, 2001.

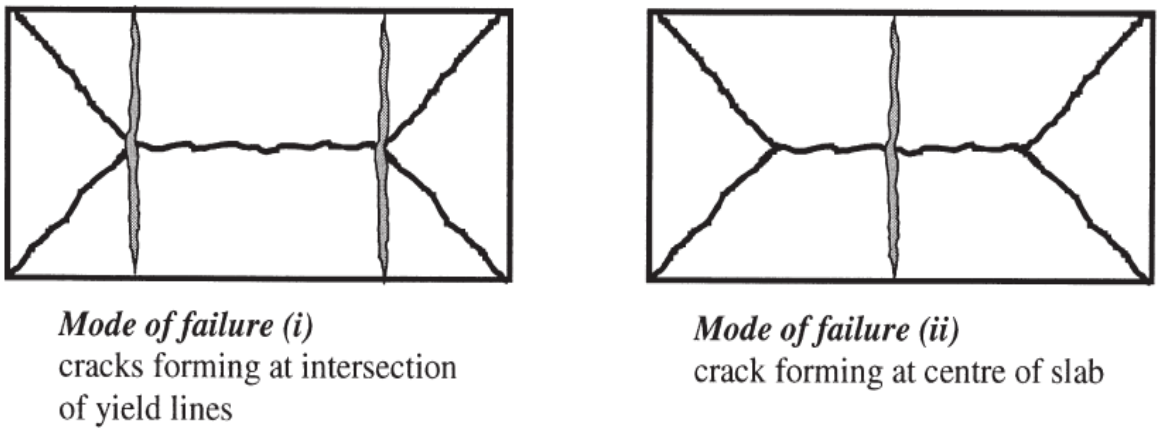

Figure 2.14: Failure models identified by Sawczuk

Sasani and Sagiroglu, 2008 studied the progressive collapse of a six-story real RC building located in San Diego under a two column removal scenario. This research included the removal of a corner column and shown that the bi-directional Vierendeel action was the dominant resisting mechanism, and withstood the failure scenario. More recently, they studied experimentally and analytically the progressive collapse resistance of an actual 11-story reinforced concrete structure after a severe initial damage Sasani et al., 2011. The initial damage was caused by two simultaneous explosions, causing the removal of four columns located on the first floor and two on the second floor perimeter. The structure resisted progressive collapse with a maximum permanent vertical displacement at the top of the removed columns of only about 56 mm. They demonstrated that such axial compressive force can significantly affect progressive collapse resistance of the structure. The shortcomings of nonlinear modeling with commonly used plastic hinges are quantified and discussed. It was shown that such a modeling method ignores axial and flexural interaction in beams and can underestimate the resisting element internal forces and successively progressive collapse resistance of the structure. Using fiber hinges in an analytical model, such interaction gave an explanation for the local and global experimental data were closely estimated. The progressive collapse resisting mechanisms primarily include the axial-flexural action of the second floor beams and Vierendeel action of the flat plate system in floors above.

Russell et al., 2015 investigated experimentally the dynamic response of reinforced concrete flat slabs after a sudden column loss. They tested seven one-third scaled reinforced concrete flat slabs under static load increases or dynamic column cases with different supports removed. They demonstrated that flat slabs, generally were able to redistribute the loading in a effective way after a column loss. Collapse due flexural failure did not occur even sizable levels of damage were detected. The results suggested that the dynamic effects due to the sudden loss of a column can be notable as deflections of up to 1.5 times the static case measured in the elastic range. It was shown that the Dynamic Amplification Factor (DAF) reduces when nonlinear damaging effects are included, which implies that conventional code based design methods for concrete flat slab structures may be over conservative.

Helmy et al., 2012, used nonlinear dynamic simulations to study the response of a 10 story structure designed according to Committee, 2008 against various column loss scenarios. The results shown that the structure did not meet the requirements regarding the progressive collapse resistance determined in UFC-4-023-03 DoD, 2008. Same authors in other research Helmy et al., 2013, found that the design of concrete reinforced structures based on ACI 318-08 Committee, 2008 met the requirements of the GSA code (GSA), 2013. Shan et al., 2019 shown the results of parametric study using FEM simulations. They found that same buildings but more storeys, be likely greater resistance to progressive collapse. More recently, Adam et al., 2020 presented the results of a full scale experimental test on a concrete reinforced building under the corner column removal scenario. In this research, they analysed the alternative load paths (ALPs) developed and computer (DAFs) based on difference with the results obtained from static analyses using FEM. Based on these results, they calibrated a nonlinear dynamic model and performed an expanded parametric study Adam et al., 2020.

2.5.2 Penultimate removal scenarios

Prior studies on progressive collapse have mainly focused on frame structures in scenarios where an interior column is removed. However, the risk of progressive collapse escalates significantly when penultimate columns near the outer edges of the structure are damaged, as these columns are subject to weaker horizontal restraints. Qian et al., 2020 conducted a static test on progressive collapse using two single-story beam-column planar substructures with flange slabs, each with either a penultimate or an interior column removed. Compared to the specimen missing the interior column, the specimen with the removed penultimate column showed greater vertical displacement at the initial small-deformation stage, thereby limiting the effectiveness of compressive arch action in resisting collapse. During the large-deformation stage, the specimen with the removed interior column displayed a significant increase in resistance, while resistance in the penultimate column removal scenario did not increase as much, as horizontal movement of the edge column reduced the rise in steel strain achieved by catenary action.

Internal forces were assessed based on strain data measured at critical sections of the slab flange beams, with results indicating that compressive arch and catenary actions were not fully developed in the specimen missing the penultimate column. Ultimately, the vulnerability assessment of the prototype reinforced concrete frame indicates a potential risk of progressive collapse, especially under large deformations if a penultimate column on the ground floor or top floor is compromised. When buildings face localized damage due to extreme loads, the floors above the compromised column deform and play a crucial role in redistributing internal forces to counteract the external load. Despite this, most experimental studies on progressive collapse have focused on single-story sub-assemblies due to high cost and laboratory space limitations. Tan et al., 2021 conducted progressive collapse simulations to identify critical parameters influencing the behavior of multi-story composite frames. Further, model size effects were examined and parametric studies were carried out to explore the impact of key variables such story count, span to depth ratio and location of column removal, on progressive collapse resistance.

Feng et al., 2022 created a multi linear model to assess the collapse resistance of moment sub

frames following the removal of a penultimate column. The findings indicate that increasing either beam depth or the top reinforced ratio in the beam significantly boosts progressive collapse resistance. Dat and Tan, 2015 explored the progressive collapse resistance of reinforced concrete buildings when a penultimate external column, located at the outer edge near the building corner, is lost. In this scenario, any catenary action in the beams and slabs bridging the lost column must depend entirely on the strength of a half perimeter compressive ring within the deflected slab area, serving as an alternative load path. Based on the findings, a straightforward conservative method for estimating the progressive collapse resistance of reinforced concrete buildings under a penultimate column failure was proposed.

2.5.3 Central removal scenarios

Pham and Tan, 2019 developed an analytical model to estimate the structural capacities of reinforced concrete beam slab systems following the removal of an internal column, incorporating the influence of tensile membrane action in the slab. The model accounts for two standard laboratory loading methods, concentrated loads and uniformly distributed loads. The example highlighted the structural enhancement potential form tensile membrane action, exceeding the yielding capacity. Thus, omitting this upper bound contribution may result in an overly conservative and costly design for progressive collapse resistence.

2.5.4 Test on buildings scheduled for demolition

Conducting full scale test under laboratory conditions is a complicated, dangerous and expensive task. For these reasons, some researchers used buildings that are close to demolition to simulate the failure of one or more columns.

Significant research on reinforced concrete (RC) structures includes studies by Sasani et al., 2007, Sasani and Sagiroglu, 2010, and Sasani et al., 2011.Sasani et al., 2007 investigated a 10-story building at the University of Arkansas in Little Rock, constructed in 1958. They observed that after the sudden removal of a perimeter column, the load redistribution was largely controlled by Vierendeel action in the frames above the column failure.

Sasani and Sagiroglu, 2008 and Sasani, 2008 focused on the 6-story Hotel San Diego in San Diego, built in 1914 2.15. After removing non-structural elements like partitions and plumbing, and then causing the failure of two columns with explosives, the vertical displacement of the slabs was minimal. This was due to the development of alternative load paths based on Vierendeel action and the role of the remaining infill walls.

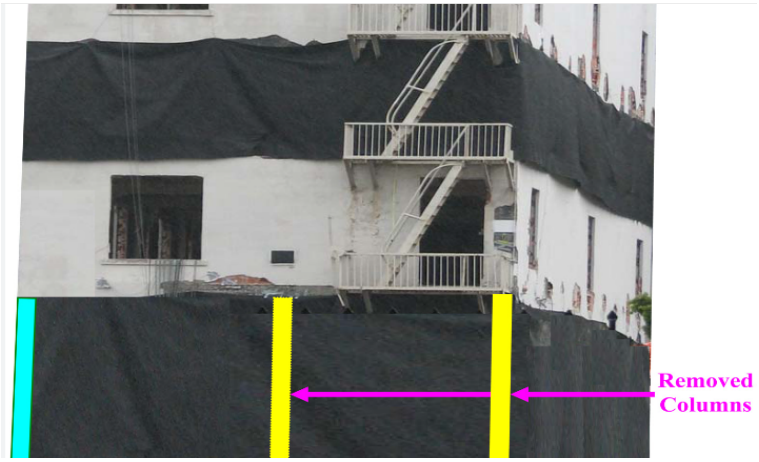

Figure 2.15: Hotel San Diego. Photo extracted from Journal of Structural Engineering Vol. 134, Nº3 (Mehrdad Sasani)

In their study, Sasani and Sagiroglu, 2010 tested the 20-story Baptist Memorial Hospital in Memphis, dating from 1956. By removing partitions and exterior walls and simulating the failure of an interior column, they demonstrated that taller buildings have better load redistribution capabilities following column failure.

Sasani et al., 2011 examined the 11-story Crowne Plaza Hotel in Houston, built in 1973. Their test simulated the simultaneous failure of four first-floor columns and two deep-beam segments on the second floor. The study found that the structure experienced minimal damage, attributed to effective load redistribution, the flexural-axial response of the deep beams on the second floor, and Vierendeel action in the upper floors.

2.5.5 Dynamic column removal

Existing literature on experimental techniques for dynamic column removal can be grouped into three main categories. Based on available experimental studies, three core categories of dynamic column removal techniques come out: quick release devices, dummy columns and explosions techniques. Progressive collapse standards suggest that, ideally, column removal should be instantaneous, with the duration kept to less than one-tenth of the period associated with the structural response for vertical motion in the bays above the removed column (DoD, 2008) (GSA), 2013). However, the timing of column removal can also be adapted to reflect the nature of the initiating threat of failure. Although instantaneous removal tends to provoke a stronger structural response, realistic test should consider the real situation. Nevertheless, following the code specified limit is crucial to fully capture the dynamic effects. The need for fully dynamic column removal ultimately depends on the specific objectives and the scope of the study. If the test simulates column loss due to a low speed impact, gradual column removal over a set period is preferable compared to an abrupt removal. In such cases, the column removal device must be able to monitor and control the timing. For explosion based techniques, column removal times are less well documented. It is important to note that the

term "column removal time" is used universally in this context, even though "release time" is more accurate for the quick release device method Kiakojouri et al., 2023.

2.5.6 Membrane action

When examining membrane action in reinforced concrete elements, it is crucial to differentiate between one-way and two-way load-bearing elements. Additionally, the horizontal boundary conditions of these elements should be considered. Figure 2.16 provides an overview of the various types of membrane action.

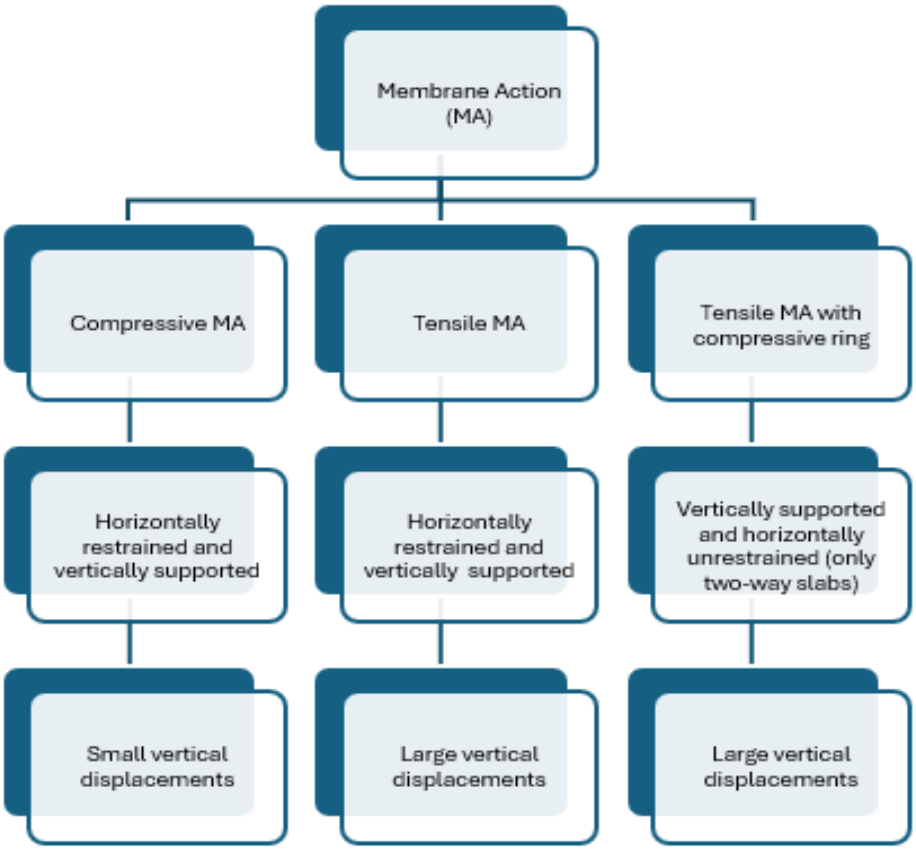

Figure 2.16: Different types of membrane action

For one-way load-bearing reinforced concrete elements, Figure 2.17 illustrates the typical load-displacement behavior for both axially unrestrained and axially restrained elements.

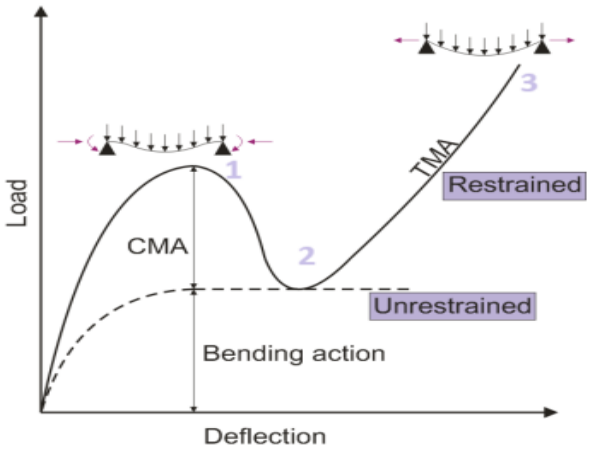

Figure 2.17: Unrestrained and fully restrained slabs response curves

The boundary conditions at the edges significantly affect the behavior of the element. When there is no horizontal restraint, or in other words, when the element is axially unrestrained, it will initially deflect until it reaches a yielding plateau. The behavior of a reinforced concrete element is influenced by its boundary conditions. For an axially unrestrained element, it will initially deflect until it reaches a yielding plateau, after which failure usually occurs due to either concrete crushing or reinforcement rupture.

In contrast, when an element is axially restrained at its supports, small vertical displacements lead to the development of compressive membrane stresses. The element's attempt to expand outward is constrained by these restraints, causing in-plane normal forces or compressive membrane forces to form. This results in a significant increase in the bending resistance of the element, as the interaction of bending moment (M) and normal force (N) leads to a higher maximum bending capacity compared to what traditional small-displacement theories or yield-line theory would predict Johansen, 1943. For less slender elements, such as reinforced concrete beams, this compressive membrane action (CMA) can substantially improve load-bearing capacity. For non-slender elements, this effect is often referred to as arching action (AA).

After reaching the maximum flexural capacity (point 1 in Figure 2.17), the element's resistance begins to decrease, and the load-displacement curve shows softening due to the reduction in compressive membrane forces. This peak load corresponds approximately with the maximum compressive membrane force, at displacement of approximately 0.5h Park and Gamble, 1999 where h is the overall depth of the element. During this phase, concrete in the compressive zones reaches its maximum strength and starts to crush under further deformation. At point 2, which usually corresponds to a vertical deflection equal to the effective depth of the element, the axial displacements reverse, causing the edges to move inward. This change results in the membrane forces shifting from compression to tension, with edge restraints countering inward movement. Cracks propagate through most of the element's thickness, marking the onset of the tensile membrane phase. During this phase, the reinforcement acts as a catenary, enhancing the load-bearing capacity under increased deflections. In literature, this tensile membrane action (TMA) is often called catenary action (CA). Looking at the slope between

Point 1 to Point 2 demonstrates the rapid development of compressive membrane force with cracking. If the reinforcement and ductility are adequate, the load-bearing capacity of the element can surpass the capacity observed in the compressive membrane phase. The final load capacity, whether in the compressive or tensile membrane phase, also depends on the element's slenderness; more slender elements tend to experience greater deformations and thus exhibit more tensile membrane action. Ultimately, the element will fail due to reinforcement rupture (point 3 in Figure2.17). Hence, the reinforcement properties, especially the ultimate strain, play a crucial role in determining the load-bearing capacity during the tensile membrane phase.

Note that the transition between the compressive and tensile membrane phases is typically observed in displacement-controlled tests, while in practice, gravity loading may lead to snap-through behavior. Key limitations to using this response mechanism in practice include the need for adequate in-plane restraint to maintain CMA and the absence of practical design methods for structures with typical span to depth ratios Punton, 2014. While in-plane restraint can often be achieved easier to accomplish within the structure's interior but more challenging along the building's perimeter.

2.5.7 Catenary Action

Catenary action refers to a secondary structural response that develops at large deflections (exceeding section's depth), beyond what is typically considered in elastic or serviceability based design. For catenary action to function as an alternative load path in structural applications, significant flexural ductility is needed, as well as specially designed connections capable of withstanding extreme rotations and combined tensile forces requirements not generally enforced by current design standards. Recent research including works by Astaneh-Asl et al., 2001, Byfield and Paramasivam, 2007, Paramasivam, 2008, indicates that achieving catenary action in typical steel structures cannot be reliably ensured by focusing solely on tensile requirements. Studies have shown that considerable rotation at connections is essential to mobilize the tying forces specified in standards like Eurocode 1; however, standard simple connections often lack the ductility necessary for the displacement needed to redistribute loads effectively.

Merola, 2009 analyzed the ductility of reinforced concrete beam-column connection, finding that the necessary rotation could be achieved. However, this process risks fracturing the top layer of reinforcement, leaving only a single layer to resist the tensile forces required for sustained catenary action. To optimize the effectiveness of catenary action, Merola suggest the use of more ductile European Grace C reinforcement.

Upon reviewing the available research, there is evident skepticism regarding the capacity of conventional steel and reinforced concrete flooring systems to sustain the required rotations in connections for safe emergency load redistribution. Studies on reinforced steel buildings appear conclusive. However, researchers investigating catenary action in reinforced concrete structures Yi et al., 2008, Gouverneur et al., 2013 highlight a significant lack of supporting experimental data, which weakens the validity of these conclusions.

2.5.8 Compressive membrane action (CMA) response

There is broad consensus on the mechanism underlying the formation of compressive membrane action (CMA). Development of compressive membrane forces is attributed to a net increase in the in-plane length along a flexural member, which is countered by lateral edge restraints Park, 1964. Initially, this process is a product of bending, where the strain compatibility within an reinforced concrete section dictates a net tensile strain at the centroid under equilibrium Vecchio and Tang, 1990. When rigid lateral restraints are present, the resulting elongation of the members is resisted by preventing lateral displacement and expansion at the supports, which induces in-plain axial compression.

Keenan, 1969 noted that with the onset of cracking and the migration of the neutral axis towards the compression face, sectional expansion becomes more pronounced. Beeby and Fathibitaraf, 2001 suggested that due to the geometric nonlinearity in the compression regions at the support and mid-span critical sections, a compression arch forms between the supports. At larger inelastic displacements, deformation is primarily due to plastic hinge rotation at the critical sections and along yield lines. Essentially, the system becomes a mechanism with two elastic segments that rotate about three hinge locations, with tow of these hinges fixed against lateral and vertical translation. Authors as Park, 1964 suggest that, at this stage, membrane forces develop further due to the spatial constraints imposed by the geometry of the system. Park and Gamble, 1999 describe this effect as a "jamming" between lateral restraints, causing the system to act as an in-plane arch or compressive membrane.

Wood, 1961 and Powell, 1966 reported that ultimate load capacities achieved through Compressive Membrane Action (CMA) reached values as high as 8.2 and 11.22 times the ultimate collapse loads predicted by Johansen's yield line theory in their respective two-way slab test specimens. Similarly, other studies, including those by Sasani et al., 2011, and Vecchio and Tang, 1990, recorded collapse loads approximately 2.0 to 6.3 times the theoretical ultimate flexural capacity in monolithic beam-slab floor systems of in-situ buildings. Keenan, 1969 emphasized that as in-plane compressive forces develop, CMA can also contribute to an increase in shear resistance. This increased structural capacity is attributed to a compressive arching mechanism, which enhances the ultimate moment capacity, reaching its maximum with peak membrane force. According to Park and Gamble, 1999 compressive membrane forces generally do not fully prevent yielding of the tension reinforcement; however, they do lead to a greater moment capacity, which aligns with the principles of conventional Moment-Axial (M-N) interaction theory. As discussed by Keenan, 1969, Beeby and Fathibitaraf, 2001, Park and Gamble, 1999, compressive membrane forces act as stabilizing in-plane forces, causing the neutral axis to shift toward the section's centroid, thereby contributing to an increase in the ultimate moment capacity.

2.6 Experimental investigation at UPM previous to this Thesis

2.6.1 Two-story concrete slab with corner column removal

2.6.1.1 Structure geometry

The structure consists of two 25 cm slabs with external dimensions of 7x7 m^2, supported on 4 columns with spans of 6.60 m. The height of the columns is 2.5 m with a 25x25 cm^2 section as can be seen in Figure 2.18, with the exception of one of those going from the foundation to the first story. This support is made by two welded UPE-100 profiles and is equipped with 3 hinges and a mechanism to block the central hinge, to guarantee stability during construction. The flexural reinforcement of the slabs is shown in Figure 2.19. It consists in a 16 mm bar mesh spaced at 20 cm placed on the bottom of face and a 12 mm bar mesh spaced at 20 cm placed on the top face.
Additionally a supplementary reinforcement for positive bending consisting in 12 mm bars spaced at 20 cm is placed on the bottom face in the column strip (1/4 of the transversal span in the vicinity of the columns). Additionally, punching reinforcement is provided as shown in Figure 2.20. Punching reinforcement consists in a total of eighteen 12 mm links. The detail used is unconventional from a theoretical point of view, since the links do not embrace the main flexural reinforcement (instead they are held together by auxiliary 8 mm bars), but this is a detail commonly used in construction and there is experimental evidence that it functions properly Caldentey et al., 2013. It was decided to use this detail to account for actual construction practices. The reinforcement of the supports consists in 4, 12 mm bars on the corners with 12 mm stirrups spaced at 10 mm in the top and bottom 50 cm and spaced at 20 cm in the central part of the supports. The stirrups are also placed at 10 cm as the column goes through the slab.

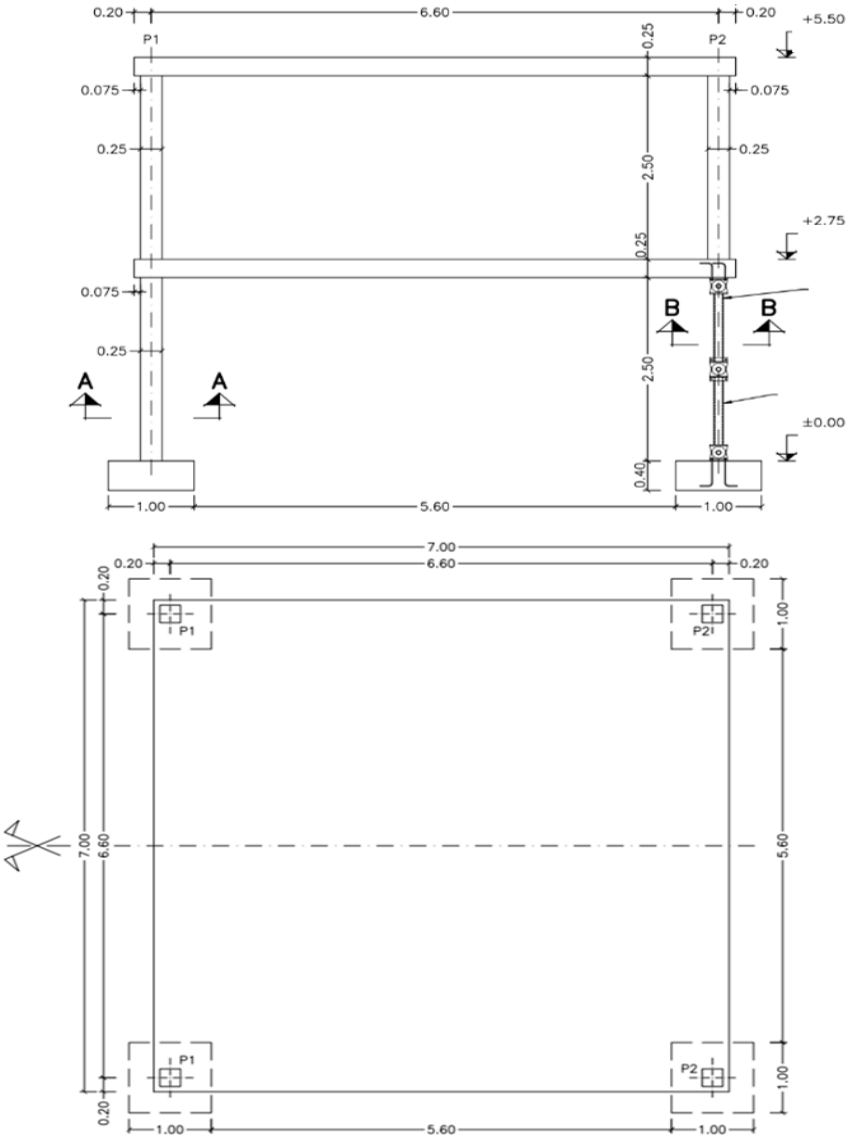

Figure 2.18: Structure elevation and plan view

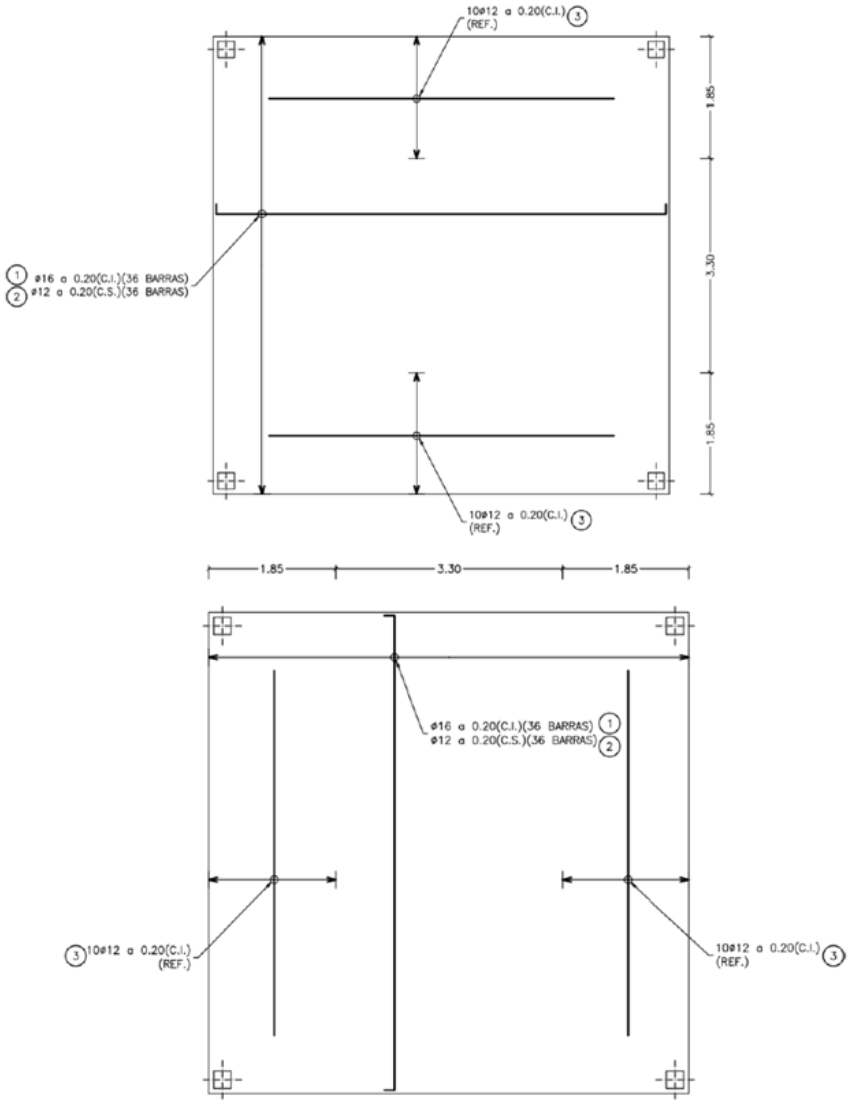

Figure 2.19: Slab reinforcement

The reinforcement of the slab was determined assuming the following loads:

- Self-weight: G1=0.25x25=6.25 kN/m^2
- Superimposed dead load: G2=1.5 kN/m^2
- Live load: Q=4.0 kN/m^2

The direct dimensioning method for slabs as described in Fomento, 2008 is used to determine the bending moments and their distribution between the column strip and the central strip. Equation 2.6.1.1 to 2.5 details the dimensioning of the flexural slab reinforcement.
Due to the uncertainties in the value of the superimposed dead load G2, a partial factor of

1.5 is applied to this load. A steel B 500 C has been assumed.

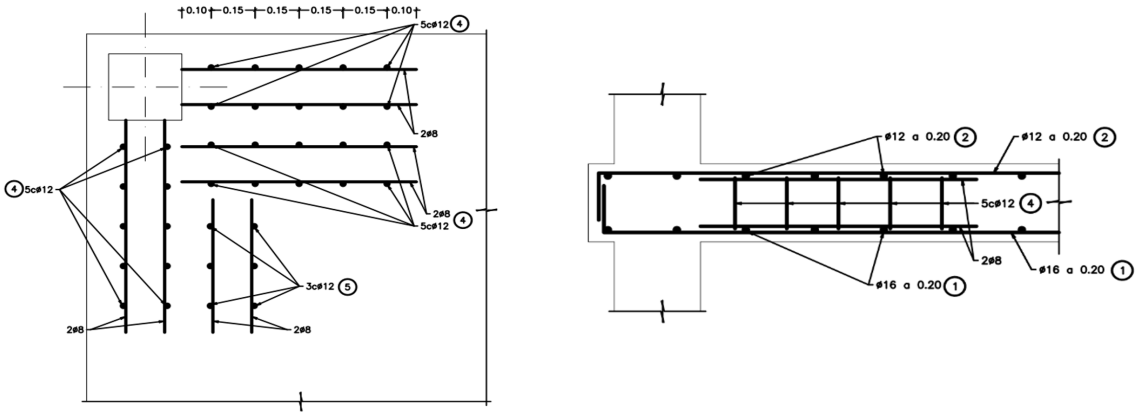

Figure 2.20: Punching reinforcement (left: plan view; right elevation)

$$M_0 = q_{Ed}\frac{L^2}{8} = (\gamma_{G_1}G_1 + \gamma_{G_2}G_2 + \gamma_{Q_Q})w\frac{L^2}{8} =$$

$$(1.35 \times 6.25 + 1.5 \times (1.5+4)) \times 7 \times \frac{6.6^2}{8} = 636.04kN \tag{2.1}$$

$$M^+_{Ed,column} = 0.6 \times M_0 = 0.6 \times 636.04 = 381.63kNm \tag{2.2}$$

$$A_s \approx \frac{0.6M_0}{0.9 \times d}\frac{1}{f_{yd}}\frac{2}{w_c} = \frac{381.63}{0.9 \times 0.2}\frac{1.15}{50}\frac{1}{3.5} = 13.93cm^2/m \rightarrow$$

$$(\phi 16 + \phi 12)/0.2 = 15.7cm^2/m \tag{2.3}$$

$$M^+_{Ed,central} = 0.4 \times M_0 = 254.42kNm \rightarrow \tag{2.4}$$

$$A_s \approx \frac{0.4M_0}{0.9 \times d}\frac{1}{f_{yd}}\frac{2}{w_c} = \frac{254.42}{0.9 \times 0.2}\frac{1.15}{50}\frac{1}{3.5} = 9.29cm^2/m \rightarrow \phi 16/0.2 = 10.05cm^2/m \tag{2.5}$$

For the dimensioning of the punching reinforcement, EN 1992-1-1:2004 CEN et al., 2004 has been used, as detailed in Equation 2.6 to 2.8

$$v_{Ed} = \beta q_{Ed}\frac{w^2}{4u_1} =$$

$$1.5(1.35 \times 6.25 + 1.5 \times (1.5+4)) \times \frac{7^2}{4(0.25 \times 2 + \frac{\pi}{2}2 \times 0.2)} \times \frac{1}{0.2} = 1.35MPa \tag{2.6}$$

$$v_{Rdc} = \frac{0.18}{\gamma_c}(1 + \sqrt{\frac{200}{d}}(100\frac{A_{s,sup/w}}{100 \times d}100{\times}25)\frac{1}{3} =$$

$$\frac{0.18}{1.15}\Big(1 + \sqrt{\frac{200}{200}}\Big)\Big(100\frac{5.65}{100 \times 20}25\Big)^{\frac{1}{3}} = 0.46MPa \tag{2.7}$$

$$\frac{A_{sw}}{s_r} = \frac{(v_{Ed} - 0.75 \times v_{Rdc}}{f_{ywe,ef} sin\alpha} u_{1d} =$$

$$\frac{(1.35 - 0.75 \times 0.46 \times 1000}{1.5 \times 0.2 \times \frac{(250+0.25\times200}{10}} 1.13 \times 0.2 = 25.91 cm^2/m \tag{2.8}$$

Figure 2.22 shows the structure built inside the lab. The dotted pattern on the side of the lower slab was used to measure the time-history of deflections along the edge of the slab during the test using Digital Image Correlation (DIC).

Figure 2.21: Full scaled test

Figure 2.22: View of the structure built inside the laboratory

Figure 2.24 shows the detail and materialization of the central hinge of the steel column. The hinge is blocked by inserting 4 horizontal 20 mm steel rods though the 21 mm holes in the top and bottom vertical plates.

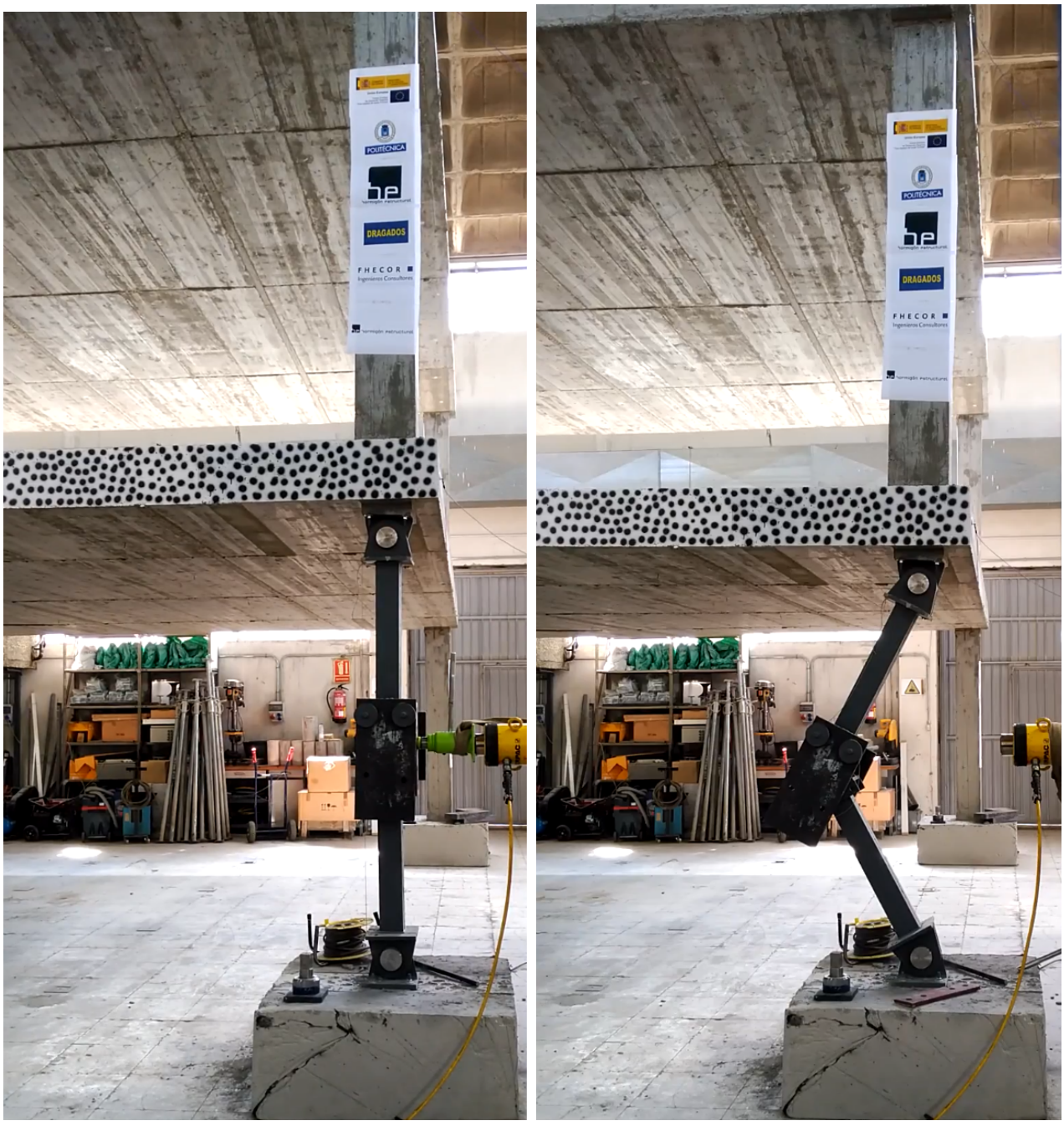

(a) Before (b) After

Figure 2.23: Hinge before and after the test

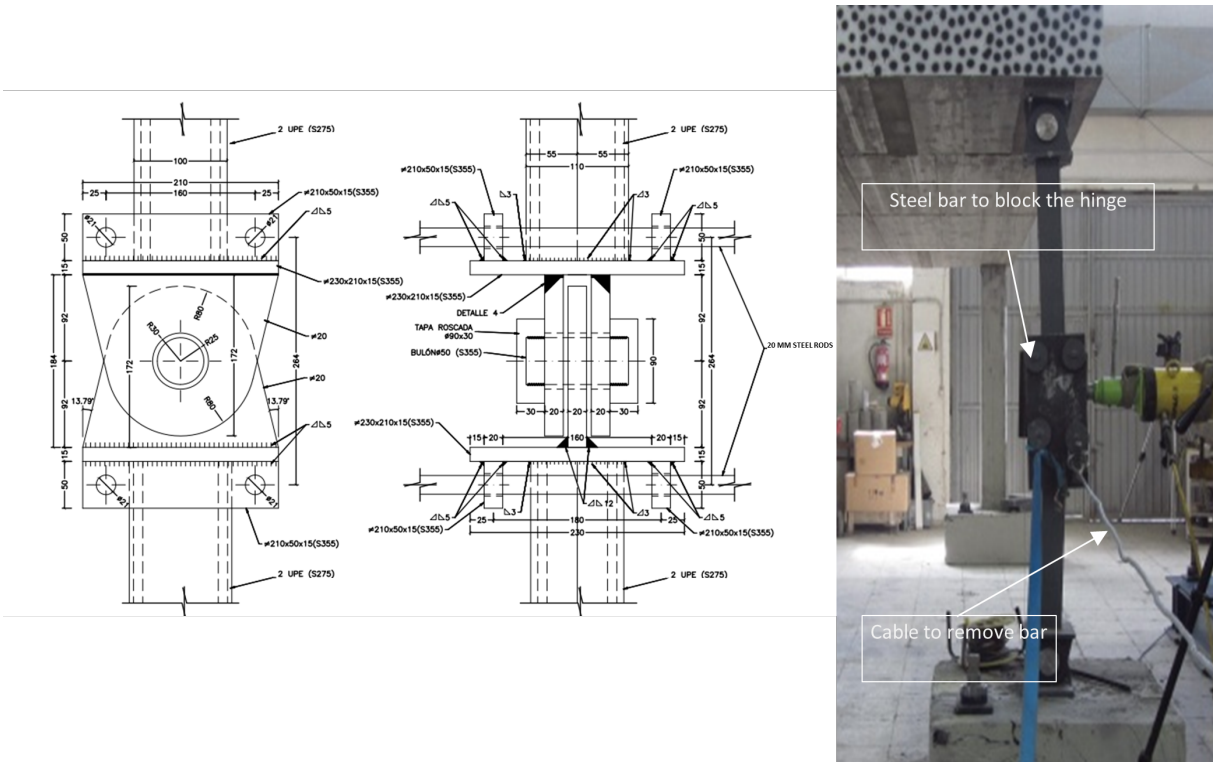

Figure 2.24: View of the structure built inside the laboratory

2.6.1.2 Material properties

The concrete was designed as class C25/30 according to Européen, 2004. The cement type used was Class S. Table 2.4 summarizes all the compressive strength tests carried out on the concrete. It was intended to test the slab at 28 days. However due to small construction delays, it was tested earlier, on May 4th 2016. At that time the bottom columns were 28 days old, the bottom slab 26, the columns supporting the top slab 23 and the top slab 20. Table 2.3 shows the estimated concrete strength of each element on the day of the test. These values were estimated by using the equations for the evolution of concrete strength with time according to Européen, 2004, assuming a value of s = 0.38 for a Class S cement, as shown in Figure 2.36. In the figure the test results are also plotted using symbols.

Table 2.3: Estimated concrete strength of the different elements at testing.

Element	Age when tested [days]	Estimated concrete strength at time of test [MPa]
Bottom Slab	26	34.44
Top Slab	20	23.71
Column supporting the bottom Slab	28	26.42
Columns supporting the top Slab	23	28.04

Table 2.4: Concrete strength

Slabs						
Bottom slab				Top slab		
Age [days]	Specimen #	Strength [MPa]	Mean values	Age [days]	Strength [MPa]	Mean values
14	1	30.22	29.27	33	25.28	25.32
	2	29.21		33	27.33	
	3	28.37		33	23.35	
89	1	35.55	35.15	91	29.3	30.72
	2	29.213		91	30.84	
	3	40.6725		91	32.02	
Colums						
Columns supporting the lower slab				Columns supporting the top slap		
21	1	23.38	24.91	36	32.91	30.51
	2	26.36		36	23.85	
	3	25		36	34.76	
93	1	30.17	30.78	91	34.53	35.09
	2	30.76		91	34.68	
	3	31.42		91	36.05	

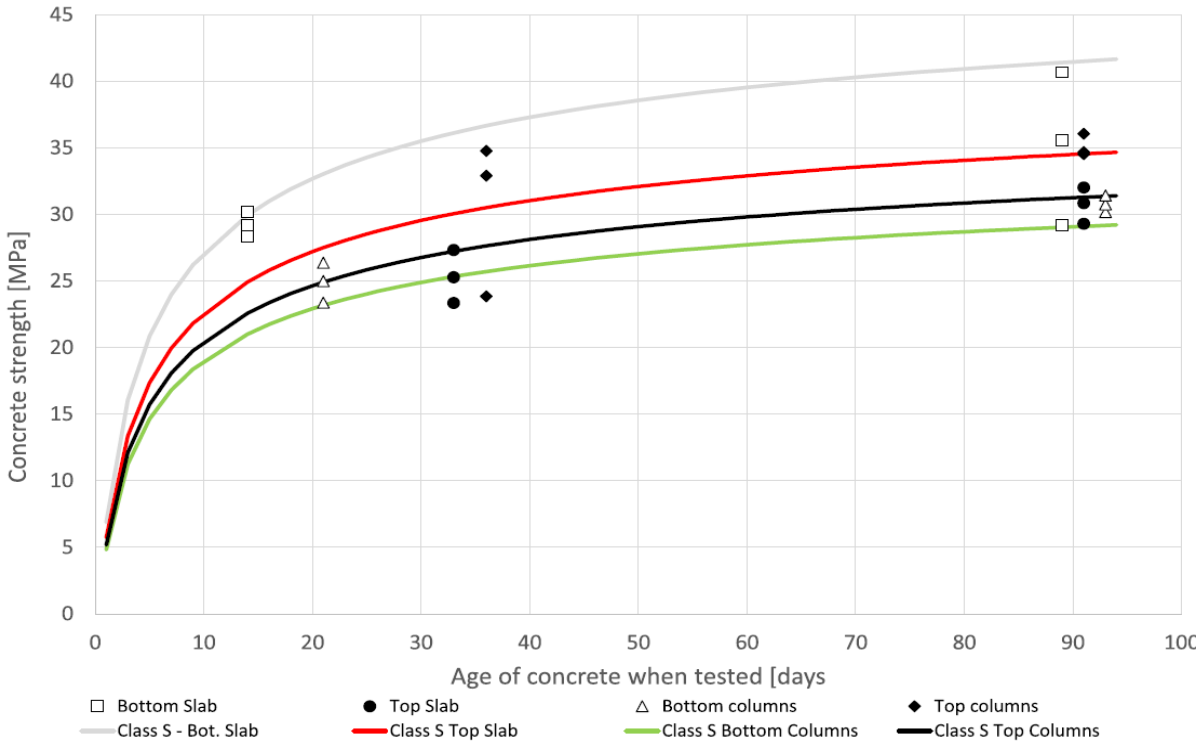

Figure 2.25: Measured concrete resistance and estimated evolution in time.

2.6.1.3 Test description

The test was carried out on May 4th, 2016. To carry out the test a hydraulic jack (yellow jack in Figure 2.24) was placed in series with a manual jack (green jack in Figure 2.24) at the point of the central hinge on the steel support. The manual jack was used to achieve good contact and a minimum level of pressure between the jack and the support. The steel support was designed so that it would be built with a slight rotation at the central hinge, so that the jack would serve as a support for the structure once the central hinge was liberated.
The four horizontal rods used to block the central hinge had a circular plates welded to them at one of the ends. It was then possible to attach a cable around the circular plate and pull the rods out using a jack placed perpendicularly to the supporting jacks. Once this operation was carried out successfully, the hydraulic jack pushed the support at the hinge, straightened the support and eventually originated its instability producing a sudden absence of support at the corner of the structure. The structure went down, at that point by approximately 22 cm. Two hours after the test, deflections had not yet stabilized, even though their increase rate was very low. It is suspected that this behavior could be related to continuing damage at the column-slab connection where inclined torsional cracks were seen to form.

2.6.1.4 Monitoring

The monitoring of the structure consisted in the following:

- Digital image correlation (DIC) which allowed to follow the displacement of one of the edges of the structure
- Accelerometers located at the corner where the column is removed on both the top and the bottom slab
- Accelerometers located at the center span of both the top and bottom slab
- A laser-scan was taken of the full structure before and after the test so that the deflection could be determined at any point of the structure
- The compressive strength tests of concrete specimens taken from the concrete used to build the columns and slabs was determined for different ages

2.6.2 Two-span concrete frame subjected to successive blast loads

2.6.2.1 Structure geometry

The structure which was tested consists of 13.60 m long, 7.00 m wide and 0.25 m thick reinforced concrete slab, supported every 6.60 or 6.475 m. For reference within the document, the span having 6.60 m will be referred to as span 1 and the span having 6.475 m will be referred to as span 2 (see Figure 2.26). The specimen was designed as an undetermined structure in order to have a more realistic representation of existing structures. The supports are of reinforced concrete. Four of the supports have a square cross section of 25x25 cm, while

the other two have a cross section of 25x50 cm. The reason for this asymmetry was that some of the FE models developed early in the works incorrectly predicted that the structural would present lateral instability. Instead of running the risk that the models might be right, it was agreed to reinforce one line of supports in order to prevent this type of failure, which eventually was shown to be the product of modelling, and not a real phenomenon.
The concrete used in the structure was a class C25/30 concrete with an aggregate size of 20 mm, a minimum cement content in the mix of 275 kg/m3 and a water/cement ratio of 0.60. This type of concrete is expected to achieve a minimum compressive strength of 25 MPa. As for the reinforcing steel, B500C rebar with an ultimate yielding of 650 MPa.
The foundation of the supports is a previously existing concrete slab. The column reinforcement was fixed to the slab by using bars anchored with epoxy resin.

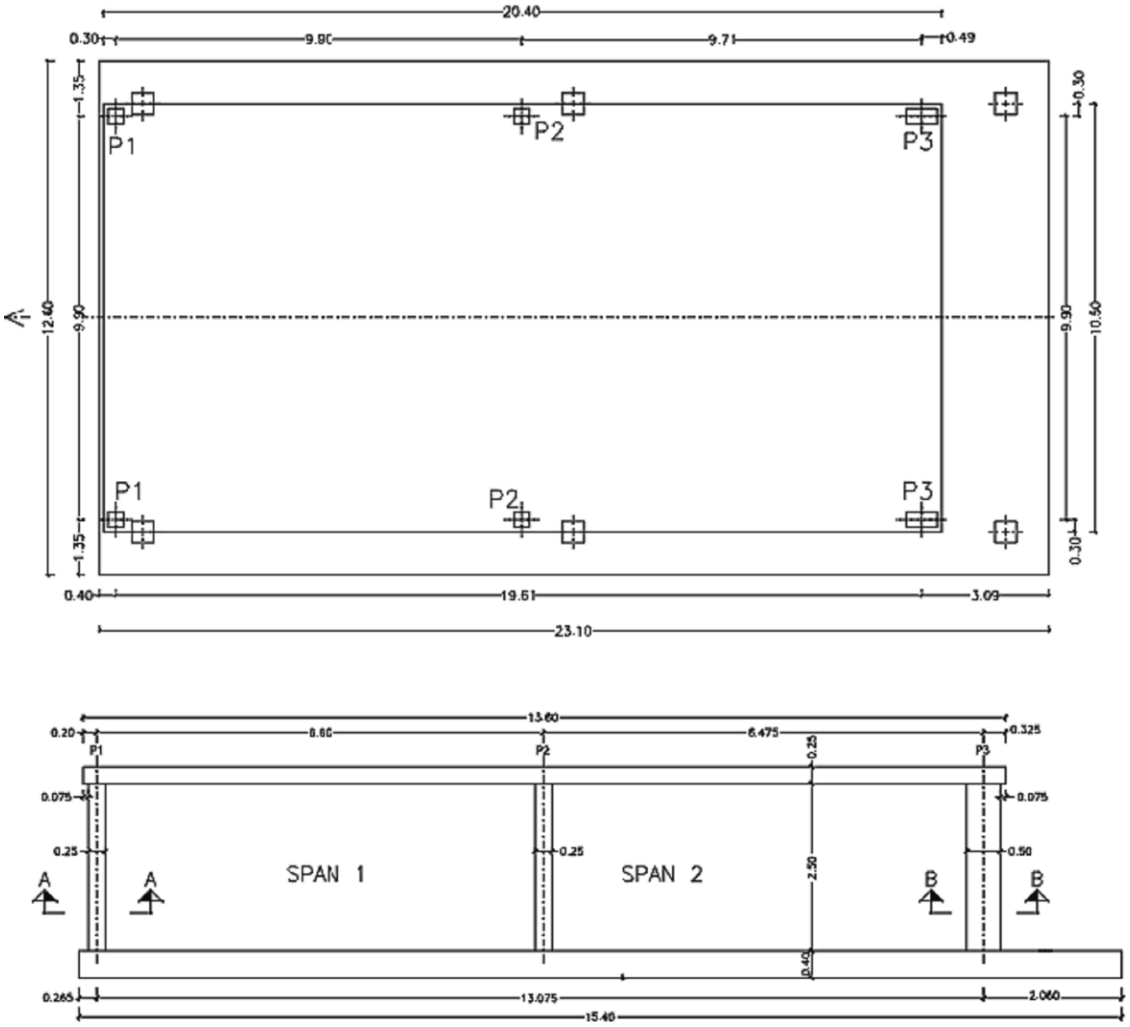

Figure 2.26: Structure geometry

2.6.2.2 Material properties

No tests were carried out to obtain the mechanical properties of the concrete so the values recommended by the EC2 were used in the numerical simulation (i.e. a compressive strength of 33 MPa).

2.6.2.3 Test description

Three different tests were performed on the same structure in order to determinate the effects of blast loads detonated on different places of the structure at different times. Table 2.5 shows the load configuration in the 3 tests performed.

Test	Explosive	Charge (kg TNT)	TNT equivalence	Standoff distance R (m)	Location	Midspan
E1	Plastic (PG2)	10	1.4	1.5	over slab	1
E2	Plastic (PG2)	20	1.4	2	under slab	1
E3	Dynamite (Riodin)	20	0.7	0.5	over slab	2

Table 2.5: Test load configuration

The explosive used in tests T1 and T2 was PG2, an RDX-based plastic explosive with a composition similar to C4 and a TNT equivalent found experimentally on a peak pressure basis equivalent of 0.8 was used in the T3 test. In all three tests the shape of the charge was roughly cubic with rounded edges and was initiated with an instantaneous detonator placed in the center of the charge.
The explosive used in tests T1 and T2 was PG2, an RDX-based plastic explosive with a composition similar to C4 and a TNT equivalent found experimentally on a peak pressure basis of 1.4. A gelatinous, nitroglycerine based dynamite (Riodin) with a TNT equivalent of 0.8 was used in the T3 test. In all three tests the shape of the charge was roughly cubic with rounded edges and was initiated with an instantaneous detonator placed in the center of the charge. For Test T1, the blast load was situated over the top of the slab, in span 1 (shown on the right in Figure 2.27).
The load was situated at a distance of 1.5 m above the surface of the slab and the explosive charge was 10 kg TNT equivalent. This first test was intended to get a first idea of the strength of the structure and was intended not to induce major structural damage.

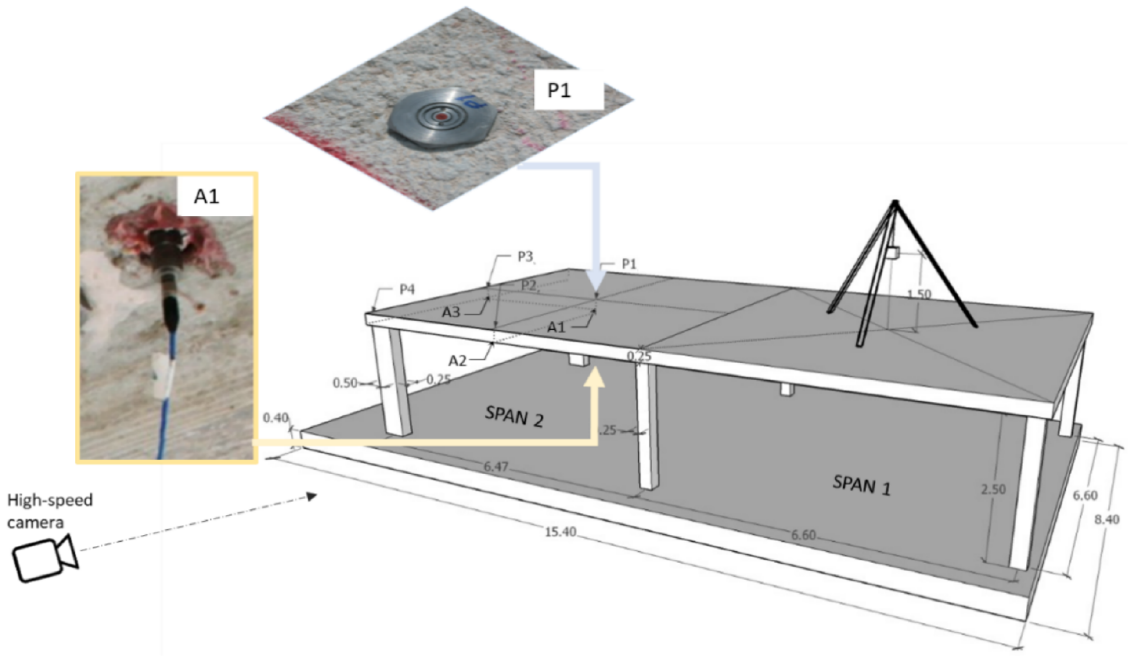

Figure 2.27: Setup Test 1: 10 kg TNT eq. at 1,5m over slab. Units in meters

For Test T2, the load was placed under the slab, 2,0 m below its lower surface in span 1. In this case, the explosive charge was 20 kg TNT equivalent (see Figure 2.28). This test was meant to simulate a typical scenario where someone would leave the explosive charge on a bench, about 0.5 m from the floor.

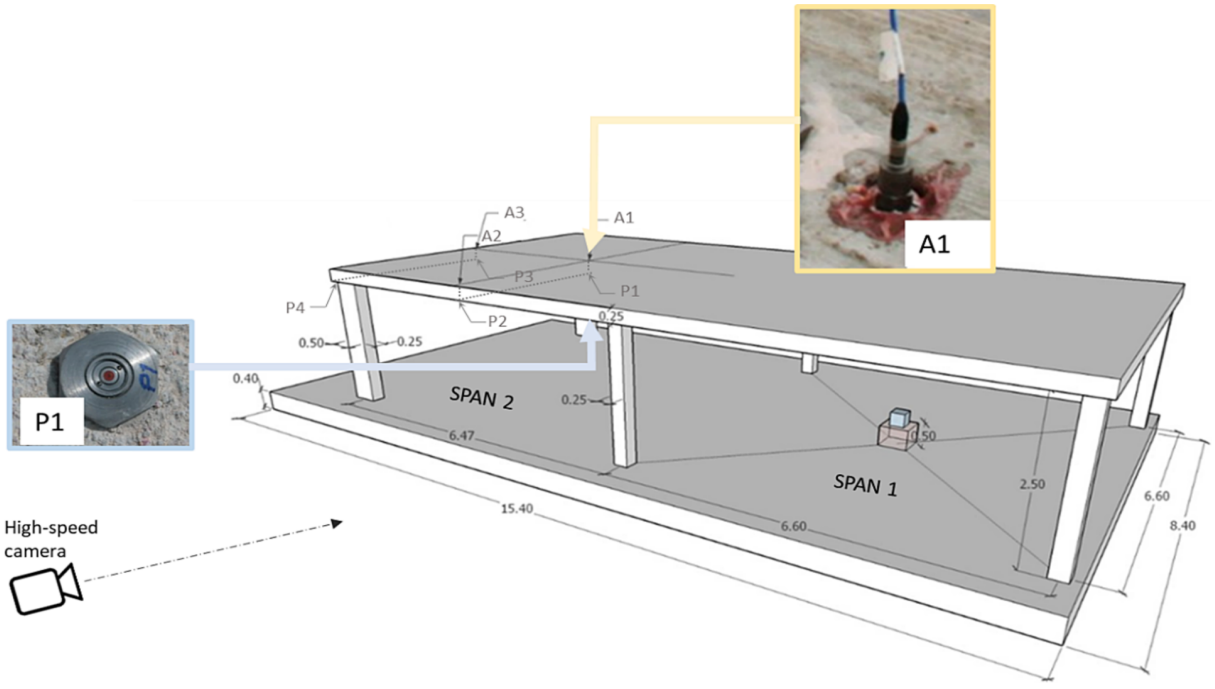

Figure 2.28: Setup Test 2: 20 kg TNT eq. at 2 m under slab. Units in meters.

For Test T3, the load was placed, over the top of the slab over the center of span 2 (shown on the left of Figure 2.29). The height of the explosive load over the top surface of the slab was 0.5 m and the load had a 20 kg TNT equivalent. This third test was again conceived as someone leaving an explosive charge on a bench 50 cm above the ground, in this case affecting the structure below.

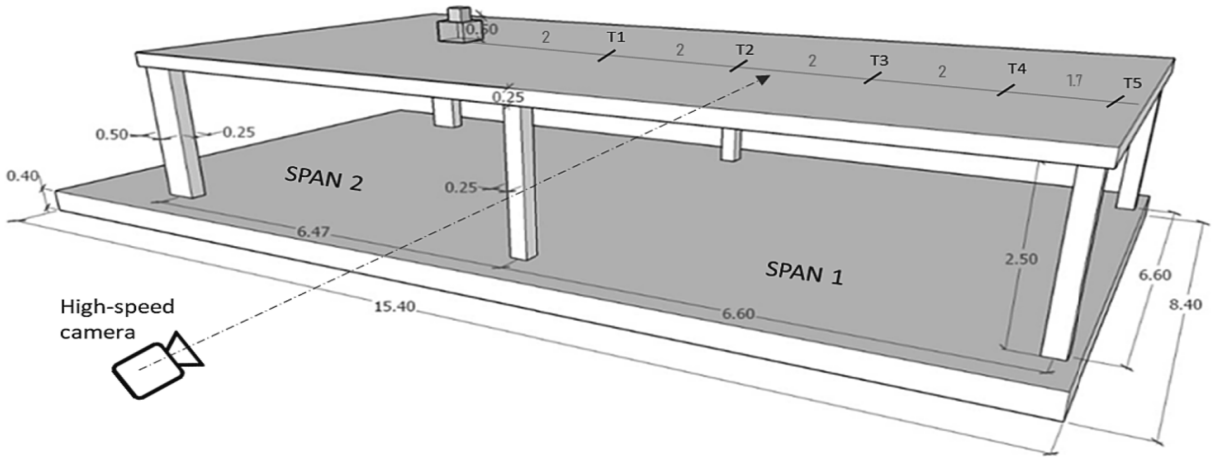

Figure 2.29: Setup Test 3: 20 kg TNT equivalent at 0.5 m over slab. Units in meters.

Once the blast test were completed, the lower portion of one of the central columns was demolished using a pneumatic hammer (see Figure 2.30). After demolition, the structure was deformed in the area of that column and reached a maximum deformation between 14 and 15 cm but maintained stability. Even though the column removal in this case cannot be said to have been sudden, this is not conceived as a problem, as the previous test of the two-story showed how limited the dynamic effects are for such a structure with only its self-weight as the applied load. However, torsional cracks appeared at the interface between the column and slab in one of the outer rectangular supports (see Figure 2.31). When the second central support was removed, the structure collapsed due to the failure of the support-slab connection.

Figure 2.30: Two-span structure: demolition of central column using a pneumatic hammer.

Figure 2.31: Cracks after one of the central supports was demolished.

Figure 2.32: Cracks close to the end of the second central column removal.

2.6.2.4 Monitoring

In order to characterize both the explosion and its effects on the structure, pressure sensors, accelerometers, laser scanner and high speed camera have been used. Table 2.6 shows a summary of the parameters measured experimentally in the 3 tests carried out. Tests T1 and T2 were monitored with pressures gauges and accelerometers. Four piezoelectric pressure sensors (P1 to P4, - see Figure 2.27 and Figure 2.28) were located in the slab with their sensor surface exposed to the blast wave. In test T1, with the load on the top slab, the pressure sensors were located on the top of the slab with the sensing surface level with the floor parallel to the forward movement of the shock, so that they recorded the incident wave. In test T2, with the load located under span 1, the pressure sensors were located on the face opposite the detonation, recording the reflected pressure on the surface. Additionally, three uniaxial shock accelerometers (A1 to A3) were fixed to the slab on the face not directly exposed to the blast.

Table 2.6: Instrumentation and experimentally measured test parameters.

Test	Pressure	Acceleration	Final displacement	Images HSC	Shockwave velocity
T1	P1,P2,P3,P4	A1,A2,A3	√	√	-
T2	P1,2,P3,P4	A1,A2,A3	√	√	-
T3	-	-	√	√	√

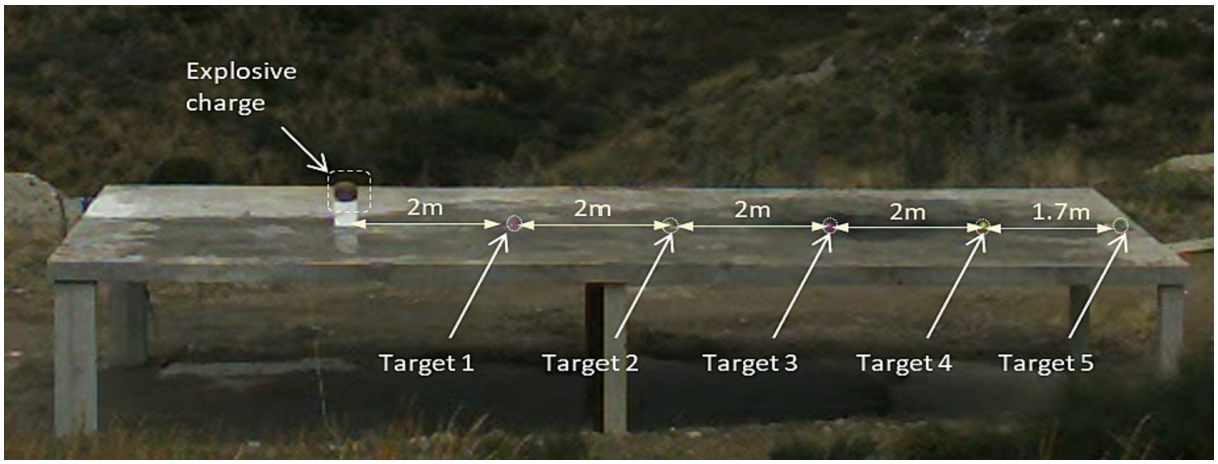

Figure 2.33: View of the high-speed camera in the T3 test with the position of the targets.

Accelerometers were screwed onto a metal support embedded in the concrete and fixed with an epoxy resin. They were placed on the face of the slab opposite to the detonation, i.e. in T1 under the slab and in T2 on the slab. A data acquisition system for pressure sensors and accelerometers with a sampling rate of 2 MHz was used. The trigger system used for the recording was the ionization of a wire placed in the detonator of the explosive charge so that the zero time corresponds exactly to the start of the detonation of the charge. All three tests were also documented by means of a high-speed camera and conventional cameras. The images obtained with the high-speed camera make it possible to evaluate the evolution of the fireball and the shock wave generated in the surroundings. The imaging speed in fps used in the three tests (6400, 4000, and 5000 respectively) was adequate to analyses the shock wave evolution. The position and orientation of the high-speed camera are shown in the diagrams in Figure 2.27, Figure 2.28 and Figure 2.29 respectively. As shown in Table 2.7, no accelerometers or pressure sensors were used in the T3 test, so in order to characterise the generated shock wave, the high-speed camera was used to measure the shock velocity. In Test T3, the high-speed camera was located in front of the structure laterally, with a view perpendicular to the longitudinal axis of the structure, in order to measure the arrival time of the shock wave at targets located at different distances on the ground. Figure 2.33 shows the positions of the targets in the T3 trial.
A laser scanner was used to evaluate the final displacements in the structure after each of the tests. By obtaining a pre- and post-scan of the structure, the data is obtained with millimetric precision. This technology makes it possible to generate a three-dimensional model of the structure as well as to obtain isoelevation curves and transverse profiles of the geometry of the structure at each measurement point.

Test	T1				T2			
Parameter Gauge:	P1	P2	P3	P4	P1	P2	P3	P4
Charge, W (kg)	10.0	10.0	10.0	10.0	20.0	20.0	20.0	20.0
Distance,d (m)	6.8	7.5	10.0	10.5	7.0	7.7	10.2	10.7
Scaled distance, z (m/kg1/3)	3.1	3.5	4.6	4.9	2.6	2.8	3.7	3.9
Incident pressure, Pso (kPa)	115.4	102.6	51.2	51.6				
Reflected pressure, Pr (kPa)					474.9	358.7	151.8	208.2
Impulse, I+(kPa,ms)	155.3	106.2	99.1	69.4	448.4	335.7	267.8	254.5
Positive phase duration, t+(ms)	4.9	3.0	5.1	4.2	4.0	2.7	4.9	4.6
Arrival time, ta (ms)	8.3	10.1	15.6	16.8	6.0	7.5	11.1	12.6

Table 2.7: Pressure Results

The pressure recorded in the T1 test can resemble the incident pressure (Pso) as the sensing surface on the ground is parallel to the shock advance. If compared to the incident pressure data for a surface type explosion, it is observed that they match quite well as it is indeed an air burst explosion with the sensors located below the triple point. The situation of the sensors in the T2 test is different and cannot be compared to a surface explosion, nor to a "free air" forming an angle with the obstacle, since the charge is located between two parallel obstacles. In the figure, the results recorded for T2 pressure are shown, and it can be seen that they are similar to those that would be obtained for a reflected wave in a surface explosion, since what happens in a surface explosion is the same as for a reflected wave in a surface explosion. Table 2.7 summarizes the measured values of pressure, impulse, duration of the positive phase and arrival time for all 4 pressure gauges for Tests T1 and T2.
Measured pressure values are compared with predictions from the Manual of the US Department of Defense, UFC3-340 DoD, 2008 in Figure 2.34 and represented against scaled distances. In this figure, pressure measurements (P) from Tests T1 and T2, arrival times of the pressure front (ta), also from Tests T1 and T2 and the shock wave velocity (u), from test T3 are represented. "The pressure recorded in the T1 test can resemble the incident pressure (Pso) as the sensing surface on the ground is parallel to the shock advance.

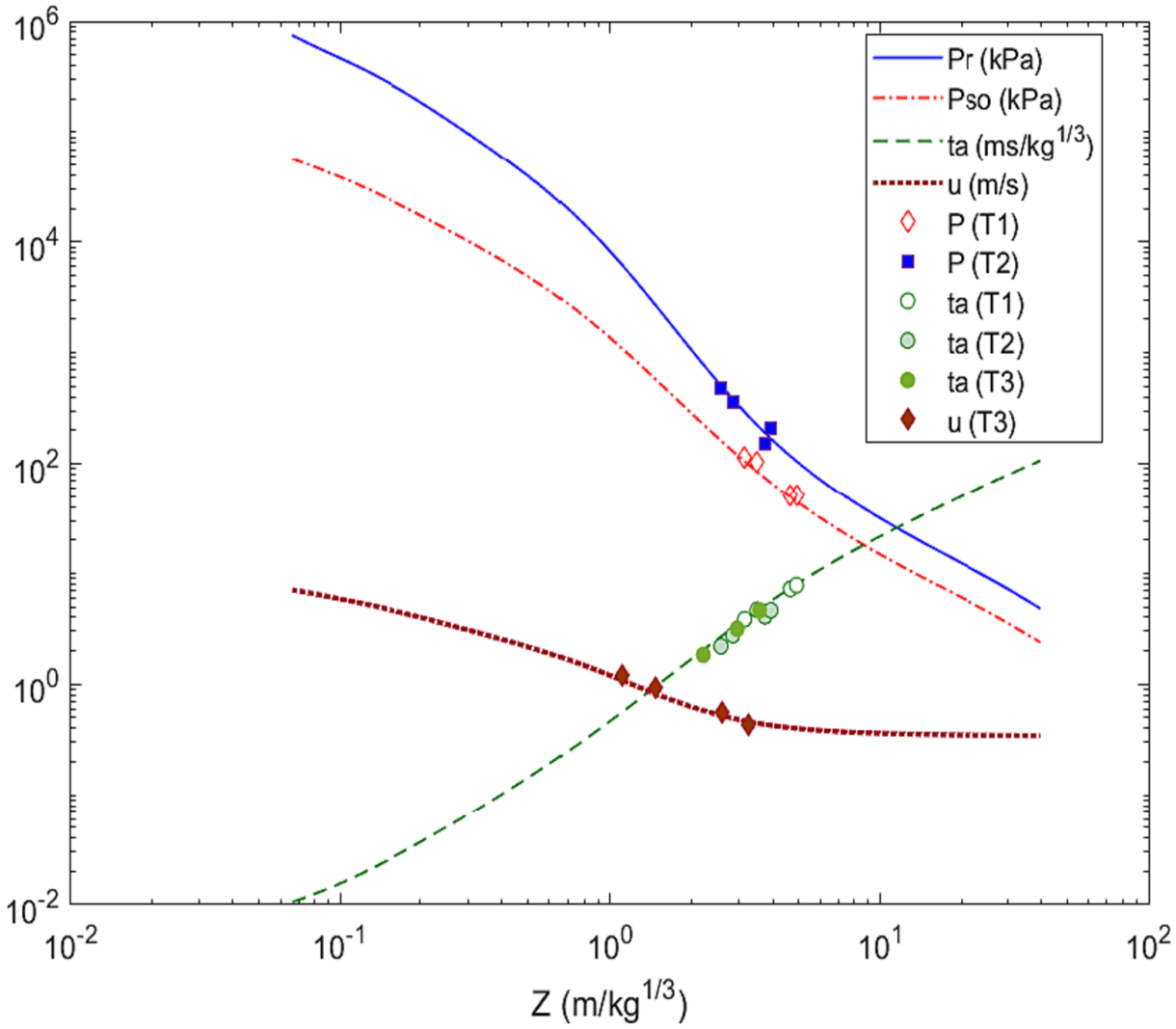

Figure 2.34: Comparison UFC 3-340 surface explosion, with experimental data.

If compared to the incident pressure data for a surface type explosion, it is observed that they match quite well as it is indeed an air burst explosion with the sensors located below the triple point. The situation of the sensors in the T2 test is different and cannot be compared to a surface explosion, nor to a "free air" forming an angle with the obstacle, since the charge is located between two parallel obstacles. In the figure, the results recorded for T2 pressure are shown, and it can be seen that they are similar to those that would be obtained for a reflected wave in a surface explosion, since what happens in a surface explosion is the same as for a reflected wave in a surface explosion.
Figure 2.35 shows the acceleration records obtained in tests T1 and T2. Table 2.8 summarises the main acceleration results including the values of the distance of the explosive load to the sensor, d, the arrival time of the pressure front to that point, ta, the peak positive acceleration recorded, ppa, the time when this peak value is reached, tppa, the peak negative acceleration recorded, pna, and the corresponding time for which this value was reached, tpna.. The accelerations recorded range from -93 to 98 g in the T1 test and from -190 to 182 g in the T2

test. The acceleration peaks, both positive and negative, have been recorded between 3 and 8 ms in all records. It is observed that the vibrations are recorded in all cases before the shock measured by the pressure sensor in the same position, as the shock travels faster through the concrete than through the air.

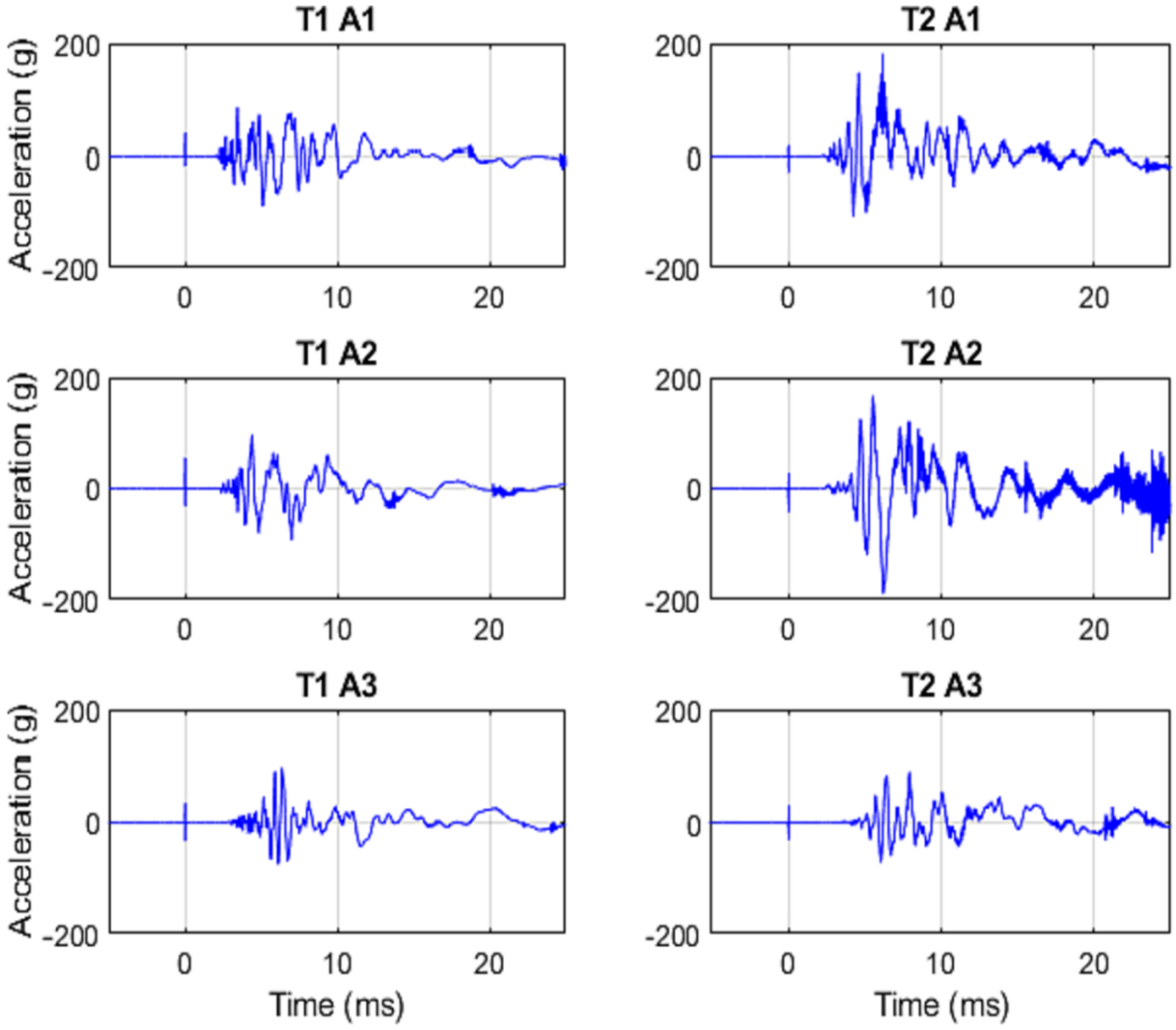

Figure 2.35: Acceleration signals Test 1 (A1, A2, A3) and Test 2 (A1, A2, A3).

Test	Sensor	Distanced (m)	Arrival time ta (ms)	Peak positive acceleration ppa (g)	Time tppa (ms)	Peak negative acceleration pna (g)	Time tpna (ms)
T1	A1	6.6	2.1	84.2	3.45	-89.9	5.12
	A2	7.4	2.26	97.1	4.42	-92.9	7
	A3	9.9	2.94	98.6	6.38	-75.9	6.13
T2	A1	6.6	2.26	181.6	6.18	-108.3	4.25
	A2	7.4	2.61	166.6	5.52	-189.8	6.21
	A3	9.9	3.09	90.7	7.9	-72	6.05

Table 2.8: Results from accelerometers fixed to the structure

In test 1, with 10 kg of TNT on the top floor, the range of the fireball is limited to span 1. A roughly spherical fireball of about 7 m diameter is observed. If the charge had been confined, the fire would have spread over almost the entire structure.
Figure 2.37-a shows the image sequence obtained in test T1 with the high-speed camera and details the time that elapses between images taking as reference (t = 0) the first photograph before the detonation. In test 2, with 20 kg on the ground floor, the extent of the fireball does not allow the shock wave to be observed in the video.
Figure 2.37-b shows 4 sequences from 0 to 15 ms in which the extent of the fireball can be observed. With this type of explosive charge, it is already necessary to consider the possible damage to the structure and its covering caused by the fire. Figure 2.36 shows the image sequence obtained in test T3 with high-speed camera and details the time that elapses between images taking as reference (t = 0) the first photo before the detonation. As mentioned above, for T3 test, five targets were positioned on the structure surface (see Figure 2.33) in order to evaluate the shock arrival times. Table 2.9 shows the arrival time results extracted from the images. Due to the fireball, only the arrival times on targets numbered T3, T4 and T5 were visible.

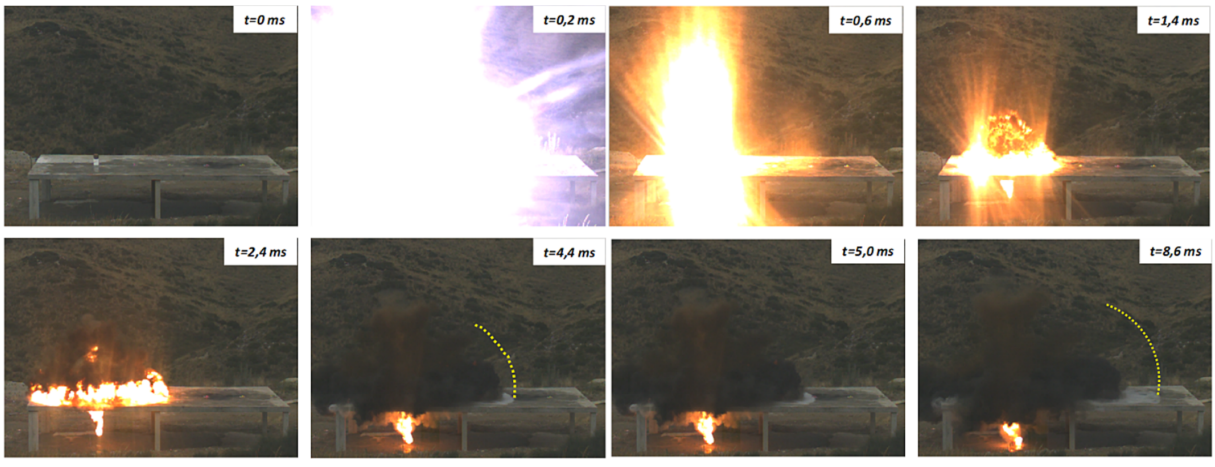

Figure 2.36: Test 3 sequence. High-speed camera.

With these data, the average shock velocity (Table 2.10) has been evaluated by assigning the mean position between the target section taken into account for the velocity calculation. The

arrival time and shock velocity parameters evaluated by analysis of the high-speed camera images in the T3 test are plotted in Figure 2.34 together with the parameters given for TNT (UFC 3-340) DoD, 2008). A good agreement is observed as with the pressure data and arrival times recorded by the sensors in the T1 and T2 tests.

Table 2.9: Arrival time obtained with High-speed camera in Test T3.

Target	Distanced (m)	Arrival time ta (ms)	Scaled distance z (m/kg1/3)
T0	0	0	
T1	2	-	
T2	4	-	
T3	6	5	2.21
T4	8	8.6	2.96
T5	9.7	12.6	3.57

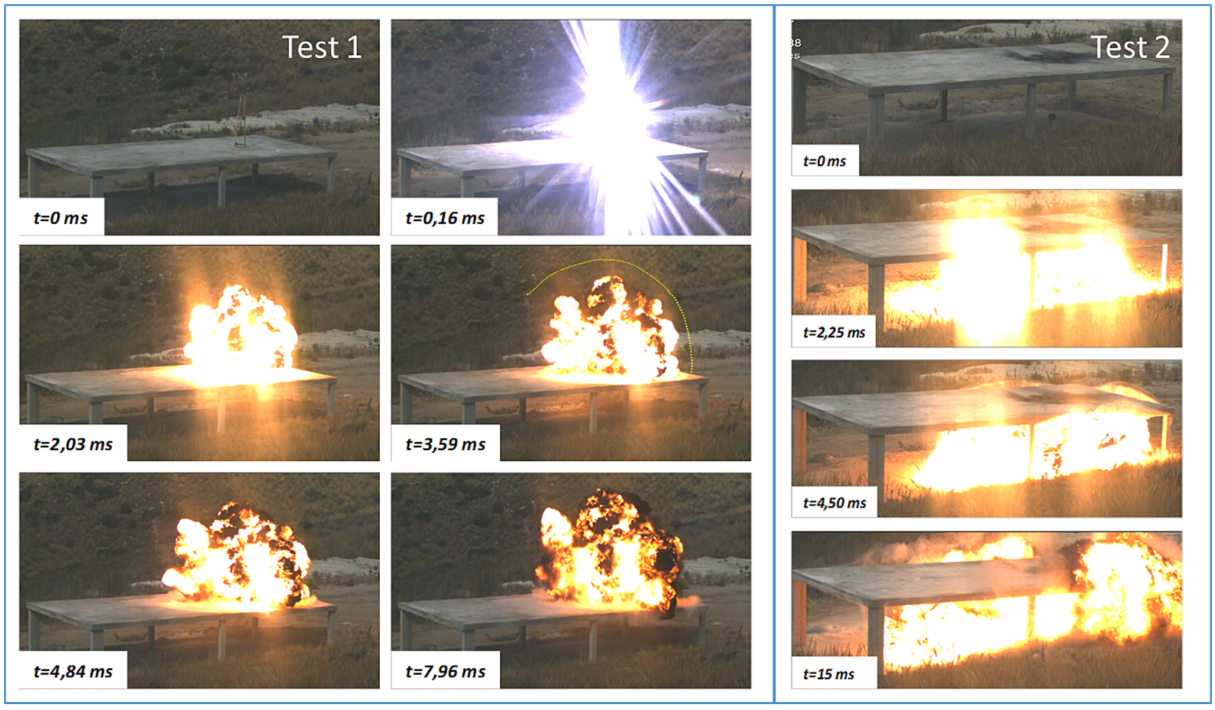

Figure 2.37: Sequence obtained with high-speed camera. a) Test 1 (yellow lines over image point out the shock wave) b) Test 2. (For interpretation of the references to colour in this figure legend, the reader is referred to the web version of this article.)

Table 2.10: Shockwave velocity obtained with High-speed camera in Test T3.

Target Section	Section distance I (m)	Time (ms)	Distance dmean (m)	Scaled distance z (m/kg1/3)	Shockwave velocity u (ms)
[T0+T3]	6	5.0	3.0	1.11	1200
[T0-T4]	8	8.6	4.0	1.47	930
[T3-T4]	2	3.6	7.0	2.58	556
[T4-Ts]	1.7	4.0	8.9	3.26	425

By using the 3-D laser scan the geometry of the structure was measured before the first blast and after each of the blasts. By subtracting the position of each point after each blast from their position at the start of the test it is possible to have an estimate of the permanent deflections inflicted on the structure by each blast as well as their cumulative effect. Figure **??** shows the displacements after each of the three successive tests, taking as a reference the original position (the one prior to test T1). Negative displacement implies downward movement. Test 2 induces an additional downwards permanent load deflection because it contributes to deteriorate the stiffness of the slab for the following reasons:

- Cracking occurs in the supports, and this reduces the embedment of the slab in hogging bending
- The second explosion produces an ascending deflection, but once the effect of the over pressure has passed gravity produces a downwards movement which is dynamic. The self-weight is therefore reapplied on the structure magnified by a Dynamic Load Factor, which contributes to increase the effect of cracking in the slab (reduction of tension stiffening effects).

At the end of the second test, the applied load is the same, but the structural stiffness is reduced resulting in a larger deflection. The values of the permanent deflections are small, less than 20 mm for the two first blasts and only 35 mm after the third blast which does inflict local damage on the structure. Note that the deflection at the perforation of the slab corresponds to the bent reinforcement which is captured by the laser-scanner. The results show that the structural solution adopted for the floor has a high degree of robustness and could withstand this range of explosive action with only local damage, without any special measures.